Sandia National Laboratories

SAND2020-10901PE

Impact of Multiscale Mineralogical and Sedimentary Heterogeneity on Mechanical Behavior of Mancos Shale

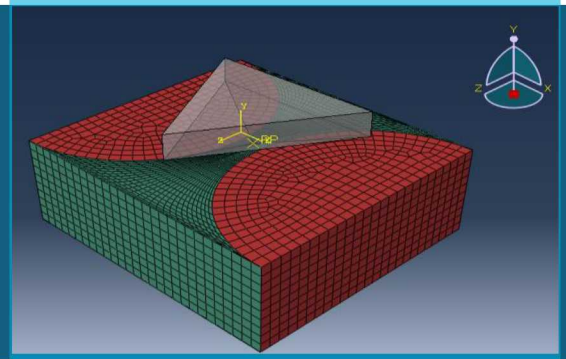

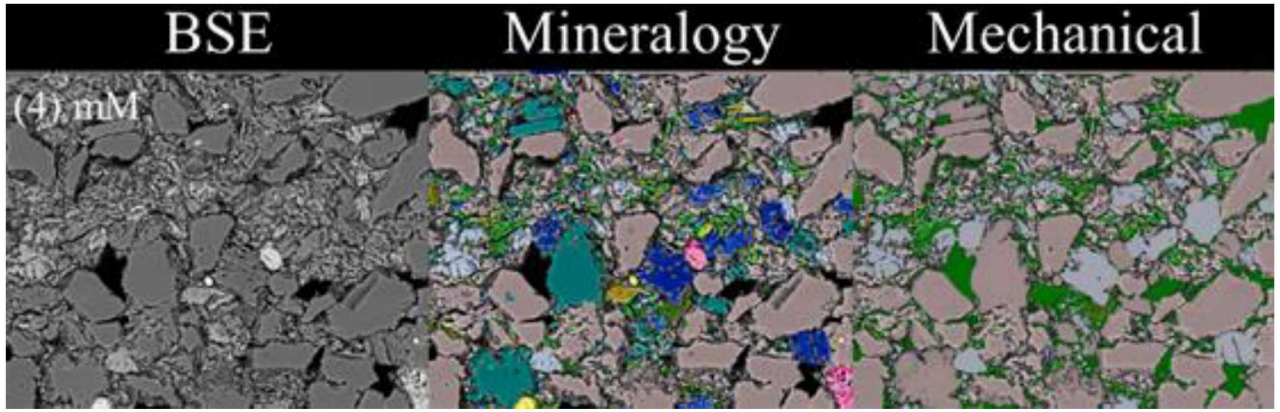

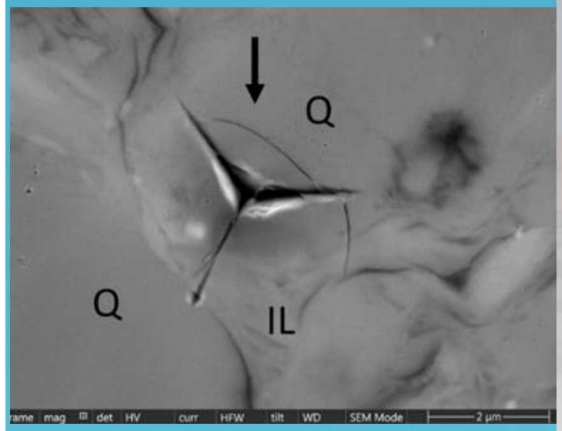

PRESENTED BY

Hongkyu Yoon (Sandia National Laboratories)

Sandia National Laboratories is a multimission laboratory managed and operated by National Technology and Engineering Solutions of Sandia LLC, a wholly owned subsidiary of Honeywell International Inc. for the U.S. Department of Energy's National Nuclear Security Administration under contract DE-NA0003525.

Acknowledgments

Laboratory Directed Research and Development program at Sandia National Laboratories

U.S. Department of Energy Office of Basic Energy Sciences, Division of Chemical Sciences, Geosciences, and Biosciences, Geoscience Program

Daniel Lizama, Thomas Dewers, Bill Mook (SNL)

Peter Mozley (NMT), Oh-Tark Kwon (NMT, currently KOGAS)

Abstract

Low permeable sedimentary rocks are important in many subsurface energy activities such as a caprock unit to provide the structural integrity for the long-term storage of injected CO_2 and unconventional oil and gas resources. Key performance of the formation such as shales is a function of the hydro, mechanical, and chemical properties of the formations with compositional and textural heterogeneity across a range of scales. In particular, mechanical properties (elastic properties, fracture toughness, anisotropy, etc.) are controlled by a variety of geologic variables, including mineralogy, cements, and organic content, and the spatial distribution of these characteristics. In this work an integrated approach of multiscale imaging, mineralogy distribution, nano-indentation, machine learning, sedimentation features, and numerical simulations is employed to investigate the impact of the micro-lithofacial heterogeneities on mechanical properties for Cretaceous Mancos Shale, a thick mudstone with widespread occurrence across the western interior of the USA. Detailed petrographic analysis results are mapped to results from axisymmetric compression and indirect tensile strength testing of this facies at the core-plug scale, and nanoindentation measurements at the micron scale. As anticipated, there is a marked difference in elastic and failure response in axisymmetric and cylinder splitting tests relating to loading orientation with respect to bedding or lamination. Shear bands and Mode-I fractures display contrasting fabric when produced at low or high angles with respect to lamination. Nanoindentation, mineralogy distribution based on MAPS (Modular Automated Processing System) technique, and high resolution backscattered electron images show the effect of composition, texture phases, and interfaces of phases on mechanical properties. A range of Young's moduli from nanoindentation is generally larger by a factor of 1 to 4 compared to axisymmetric compression results, showing the important effect of pores, microcracks, and bedding boundaries on bulk elastic response. Together these data sets show the influence of cement distribution on mechanical response. Variations in micro-lithofacies are first-order factors in determining the mechanical response of this important Mancos constituent. This work allows us to make more accurate prediction of reservoir performance by developing a multi-scale understanding of mudstone response to subsurface energy activities.

Sandia National Laboratories Overview

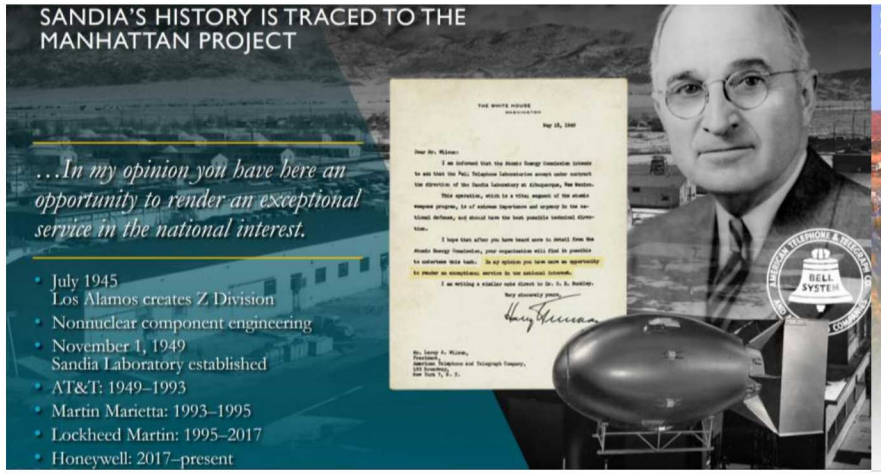

SANDIA'S BUDGET and WORKFORCE

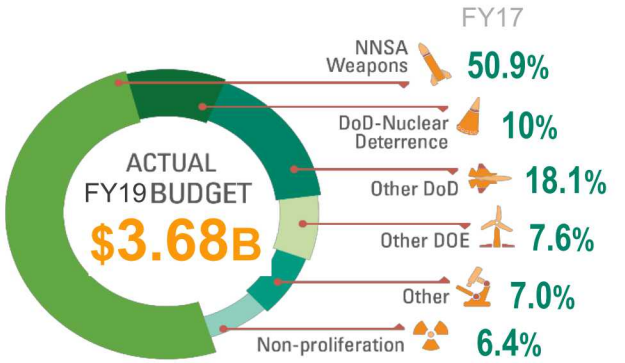

14,014 Sandia Employees NM - 12,371

7,117 Advanced Degrees NM - 6,131

1,912 Hires NM - 1,645

SANDIA Research Foundations & Mission Foundations

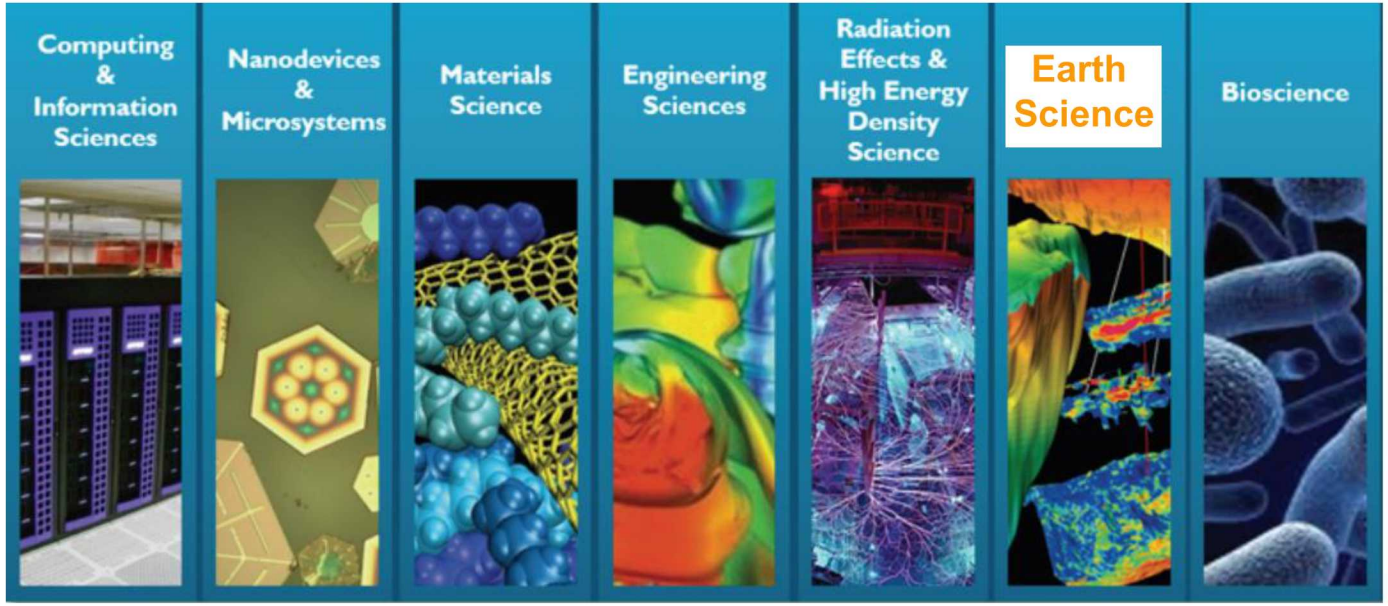

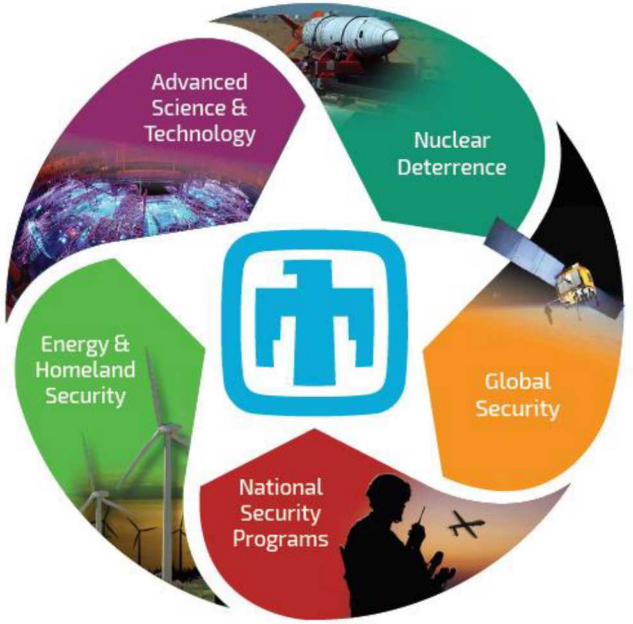

Shale as a Caprock and Unconventional Resource

Geological Carbon Storage
DOE EFRC CO2 center (FY09-18)

CO2 flow & Induced Seismicity

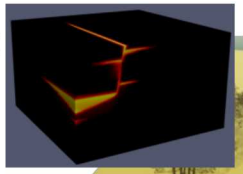

Capillary & buoyancy controlled CO_2 migration

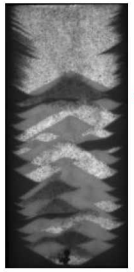

Mineral trapping

Chemo-mechanical Processes

Mechanical & Fracture Flow
SNL Geomechanics LDRDs

Wellbore Breakout (Choens et al., JGR 2019)

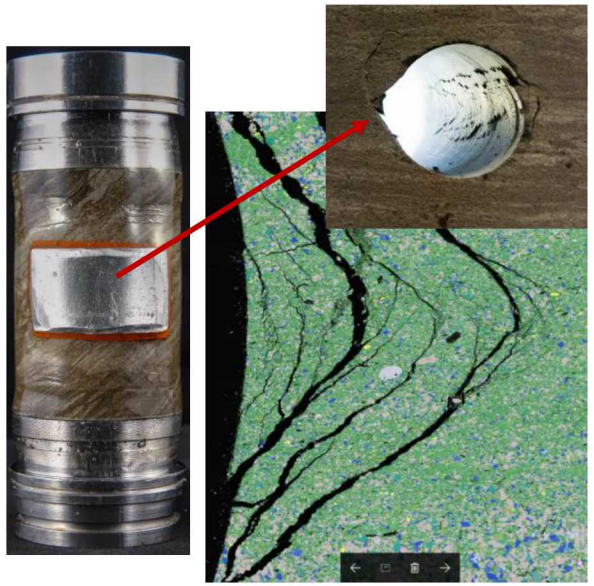

3D printing for Permeability control with proppants (Martinez et al., SAND 2017)

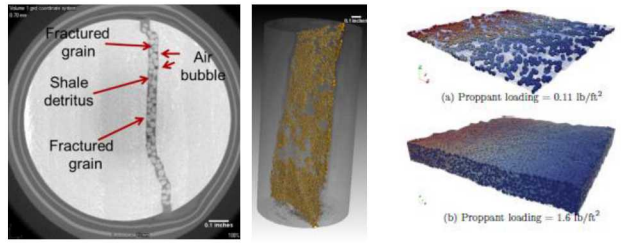

Proppants in a fracture (Bolintineanu et al., 2017)

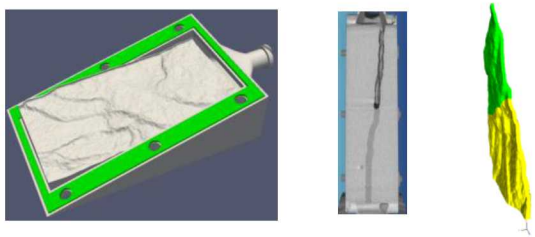

► **Sustaining large storage rates**, of order gigatons of CO_2 per year in the US, for decades with storage integrity and without compromising other subsurface resources

► **Using pore space with unprecedented efficiency**, placing CO_2 so that it occupies half of the reservoir volume, rather than the typical current estimate of less than 5 %

► **Geomechanical Experimental Capabilities under pressure, temperature, environmental conditions:** State of the art geomechanical experimental capabilities

► **Sandia Internal LDRD projects, DOE BES, FE, EERE, NE programs, Industrial projects**

Motivations & Objectives

Impact of micro-lithofacial heterogeneities on mechanical properties for Cretaceous Mancos Shale

- Mechanical properties of fine-grained sedimentary rocks (shale and mudstone) are important for shale resource recovery, geological carbon storage, and nuclear waste disposal
- Develop a novel workflow for integrating high resolution mineralogy mapping, multiscale nanoindentation analysis, and modeling
- Link geological attributes to microscale mechanical properties of Mancos shale

Clay-rich area,
256 (16x16 grid)
nanoindentations

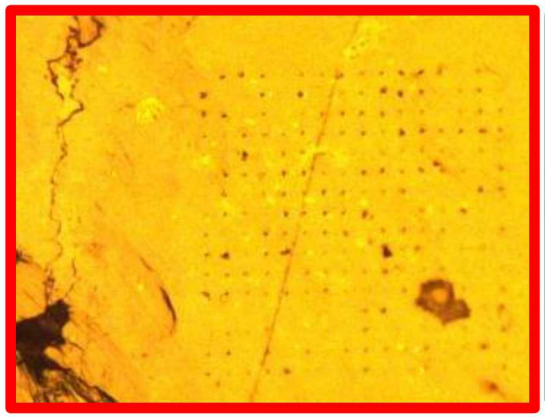

Optical image

Load-displacement

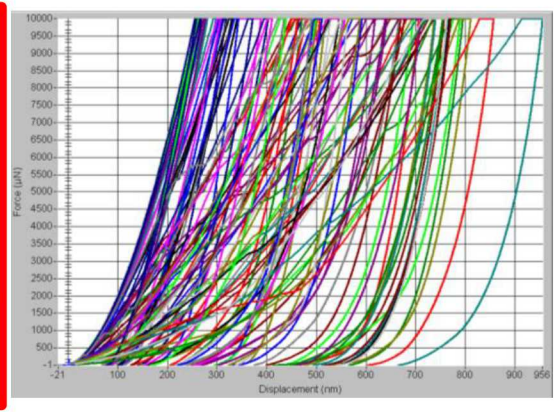

Reduced Young's Modulus

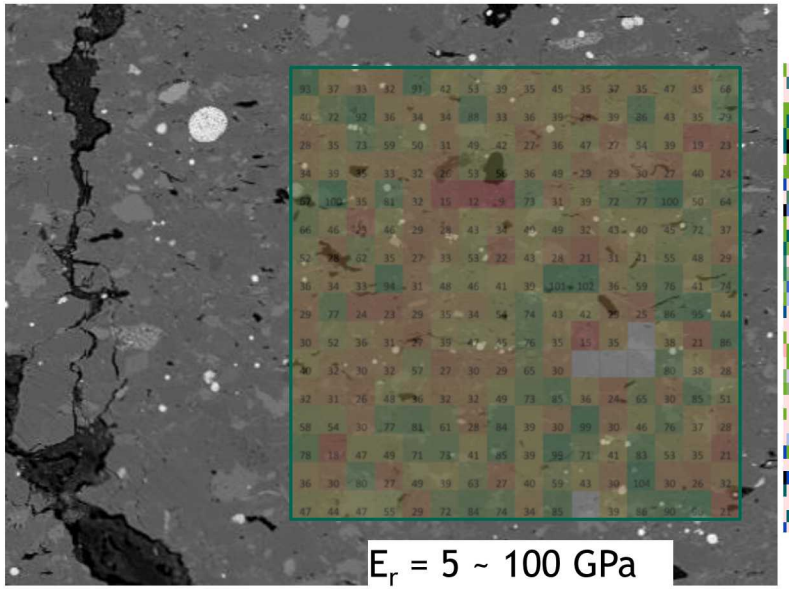

Mineralogy mapping

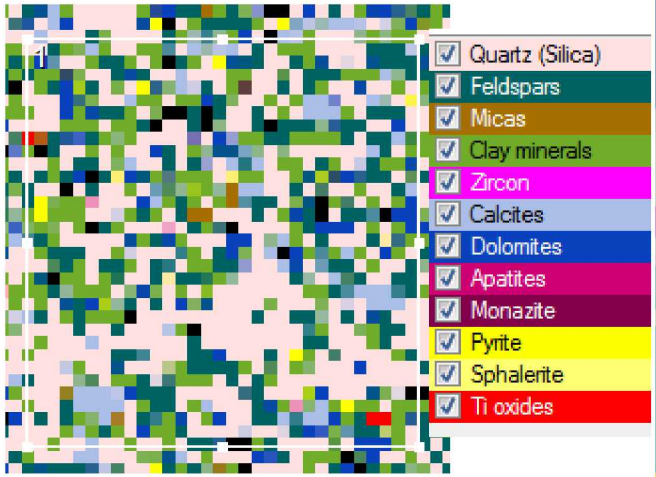

Integrated Approach

- **40 cm diameter core of Mancos shale**
  - Interlaminated fine/medium/coarse mud (fM/mM/cM), medium sand (mS), and sandy coarse mud (scM)
  - 1-3 mm laminae
  - Parallel lamina, wavy lenticular lamina, ripple forms, and bioturbation
- **Mineralogical and textural characterization***
  - Macroscopic
  - **Optical petrography/microscopy**
  - Micro-CT
  - **XRD/X-ray Microprobe**
  - **Small Angle Neutron Scattering**
  - Focused Ion Beam-SEM
  - **Back-Scattered Electron Microscopy**
  - **MAPS Mineralogy (Mineralogy mapping)**
- **Mechanical Experiments**
  - Uni-/Tri-axial compression (1x2")
  - Brazilian Test (1x0.5")
  - **Nanoindentation**
- **Computational modeling**

* highlighted in yellow for this presentation

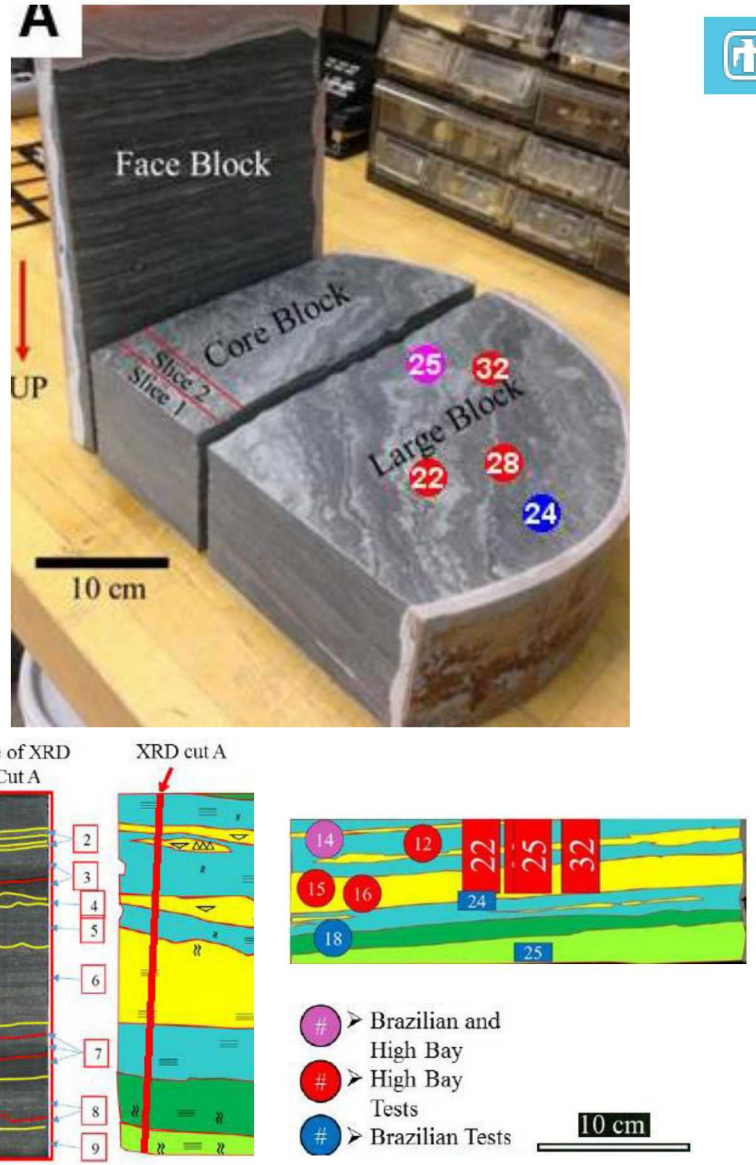

A. Photo of 40cm diameter core sample
B. Locations of small core and thin section samples for characterization and experiments

Yoon et al. (AAPG, Memoir 120, Chap. 8, 2020)

- **Mineralogical and textural characterization**
  - Macroscopic
  - **Optical petrography/microscopy**
  - Micro-CT
  - **XRD/X-ray Microprobe**
  - **Small Angle Neutron Scattering**
  - Focused Ion Beam-SEM
  - **Back-Scattered Electron Microscopy**
  - **MAPS Mineralogy**
- **Mechanical Experiments**
  - Uni-/Tri-axial compression (1x2”)
  - Brazilian Test (1x0.5”)
  - Nanoindentation
- **Computational modeling**

Multiscale characterization of nano-porous geomaterials

Macroscopic and microscopic lithofacies (optical petrography)

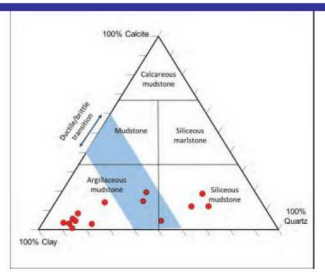

Optical and Confocal Microscopy

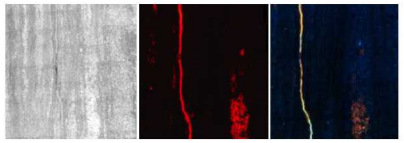

3D multiscale microCT
X-ray probe and QEMSCAN for mineralogy

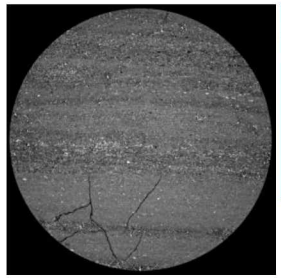

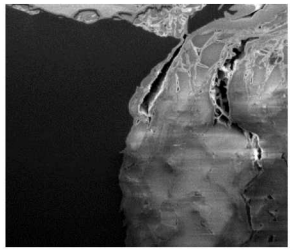

mSEM, Maps Mineralogy

Focused-Ion Beam & Broad-Ion Beam for milling

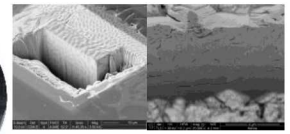

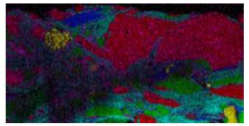

SEM, EDS

Electron Microscopy

(Ultra) Small Angle Neutron Scattering

1 m | 10^{-3}m | 10^{-6}m | 10^{-9}m

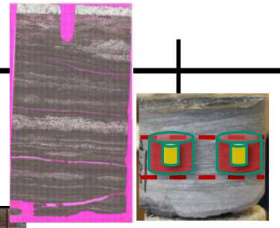

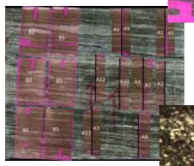

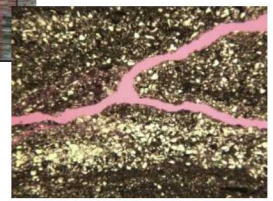

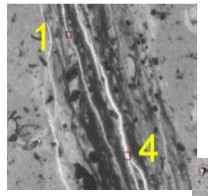

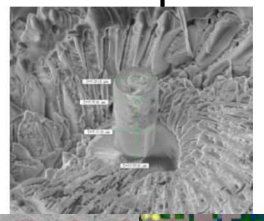

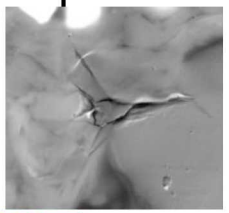

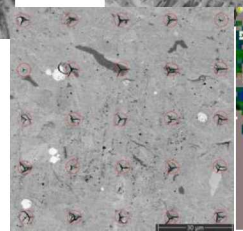

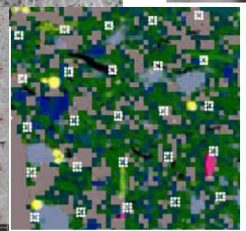

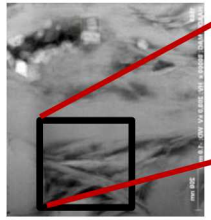

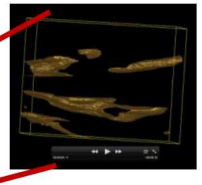

MAPS Mineralogy

- **SEM-based Modular Automated Processing Systems (MAPS): mineralogical measurement, analysis, data integration**
  - Collection, overlay and re-registration of multiple images from different modalities
  - SEM-EDS, optical, CL, EBSD
  - QEMSCAN measurement algorithm
  - Developed by a formerly FEI (now Thermo Scientific)
- **Mineral identification**
  - Spectral matching
  - Each pixel – single/multiple minerals
  - Elemental substitutions
  - Simultaneous mineral element and count maps

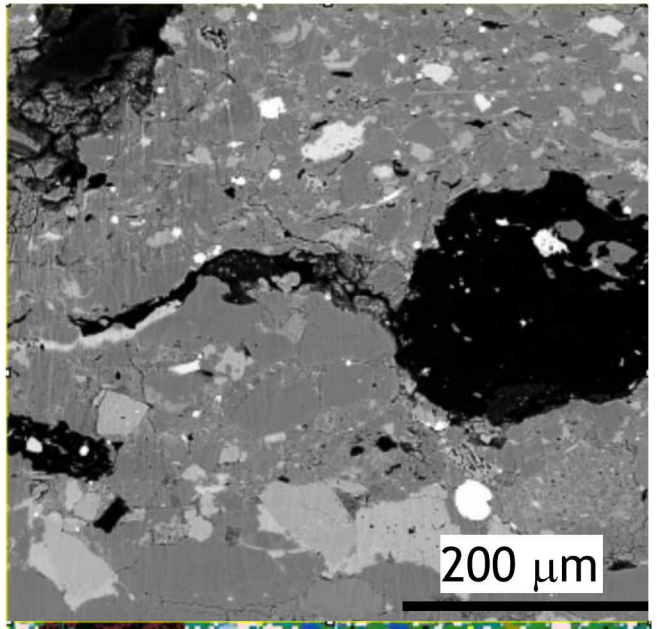

← BSE image

Ion-milling polished Mancos sample (1 inch diameter)

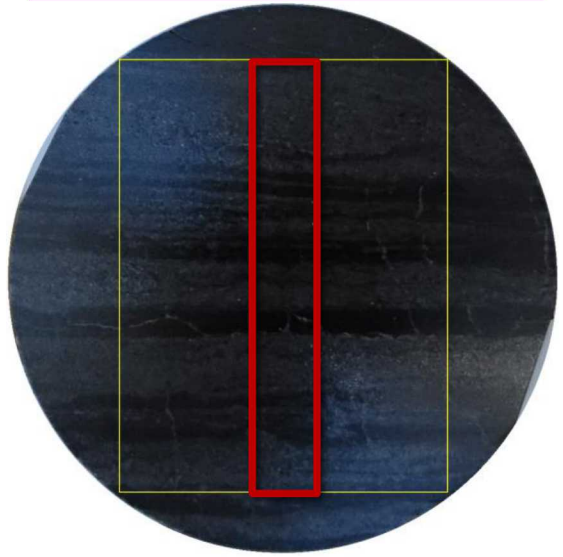

Yellow Box (1.45 x 1.98 cm): BSE @ 1µm & MAPS @ 10µm
Red box (0.18 x 1.98 cm): BSE @ 0.2µm & MAPS @ 2µm

Spectral matching for multiple minerals @ pixel

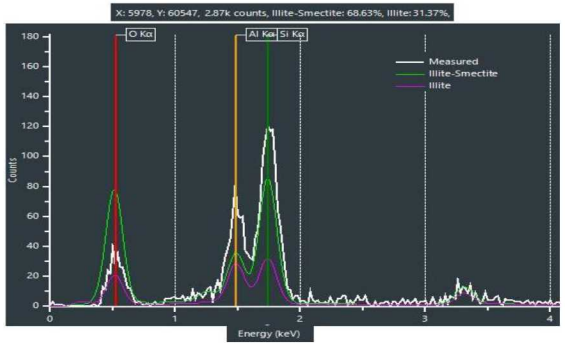

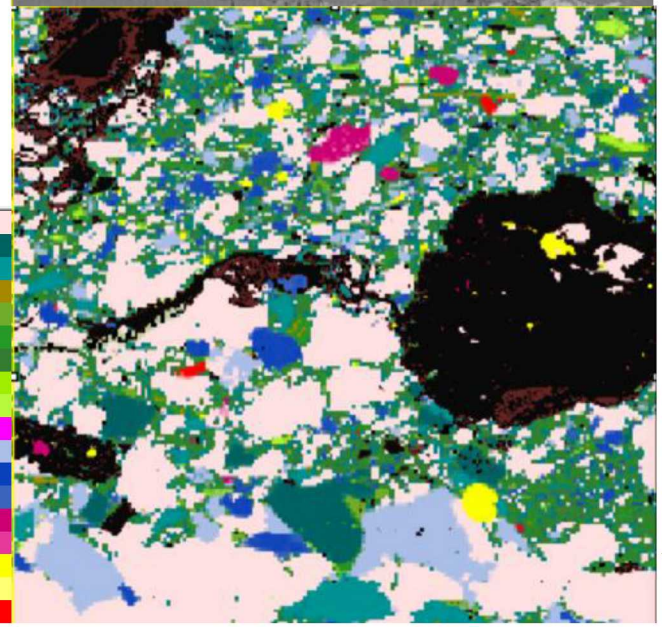

← Mineralogy map (black for organic/crack)

Sample Prep & Analysis

Ion-milling polished sample
(1 inch diameter)

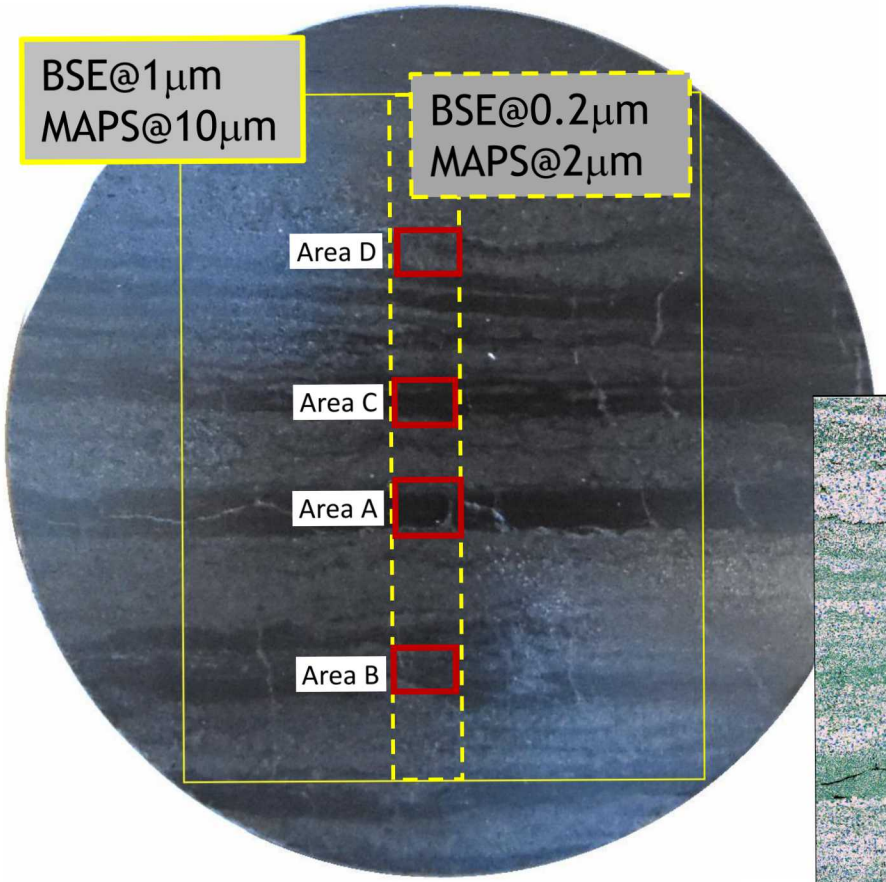

Nanoindentation Area

Hysitron Modulus Map using nanoDMA III

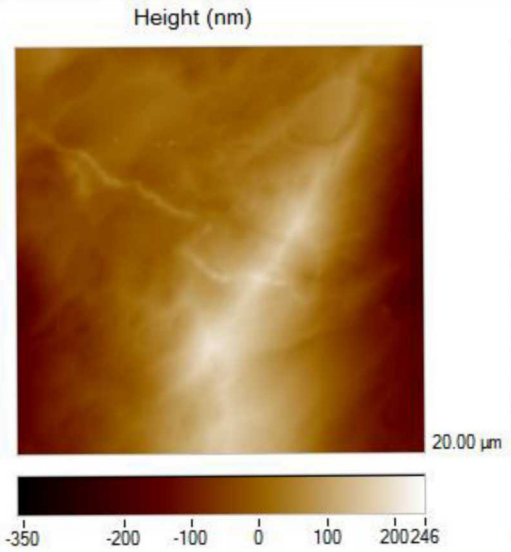

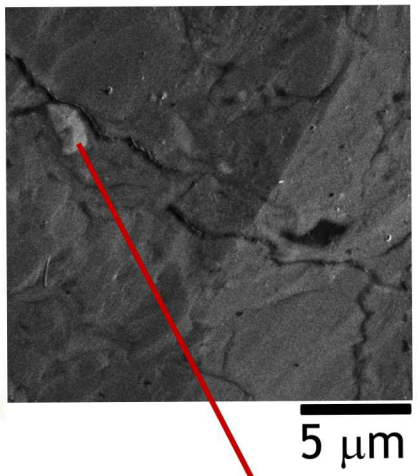

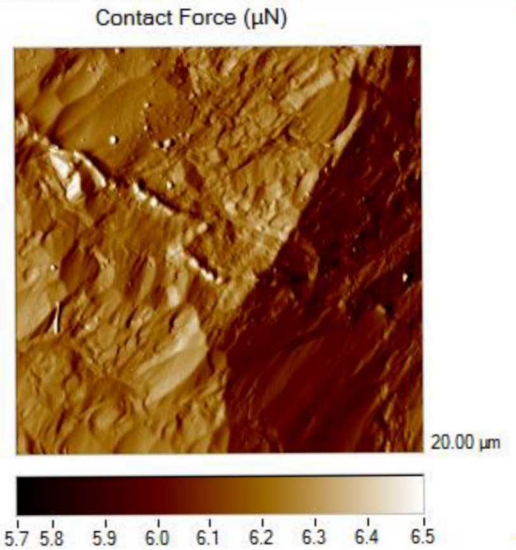

MAPS data analysis

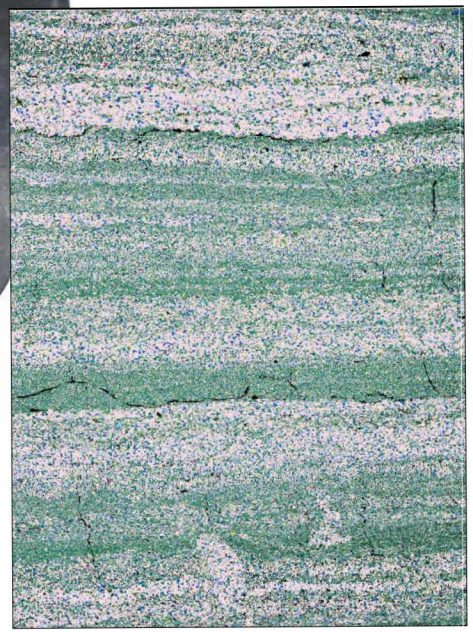

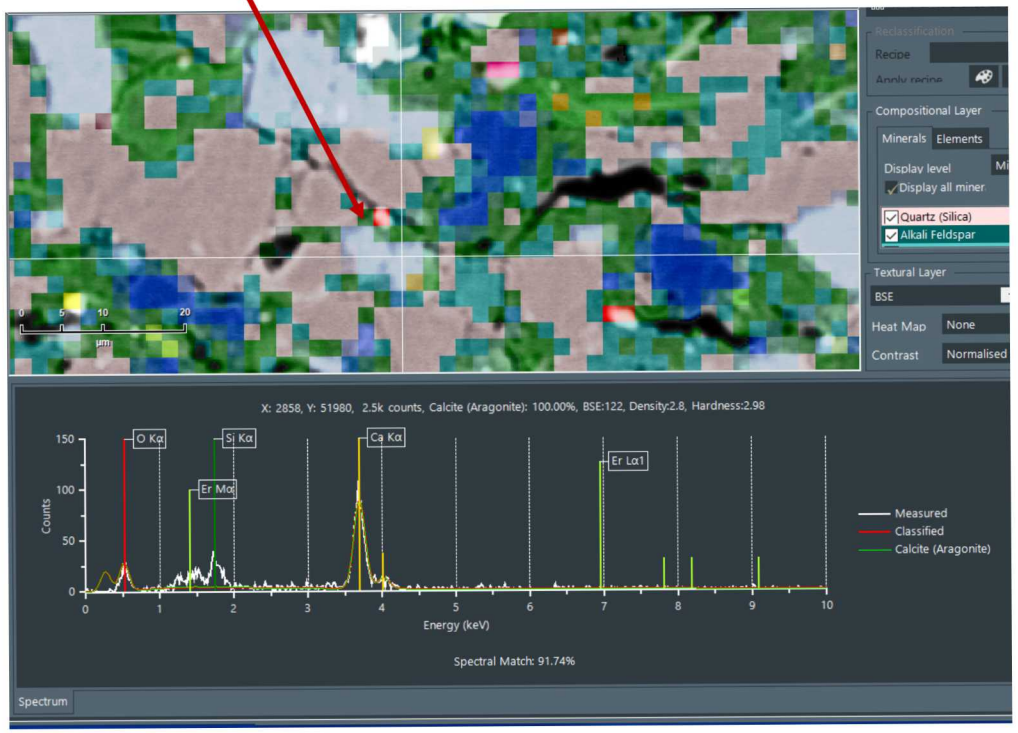

Mineralogy Mapping: Scale/methods dependent

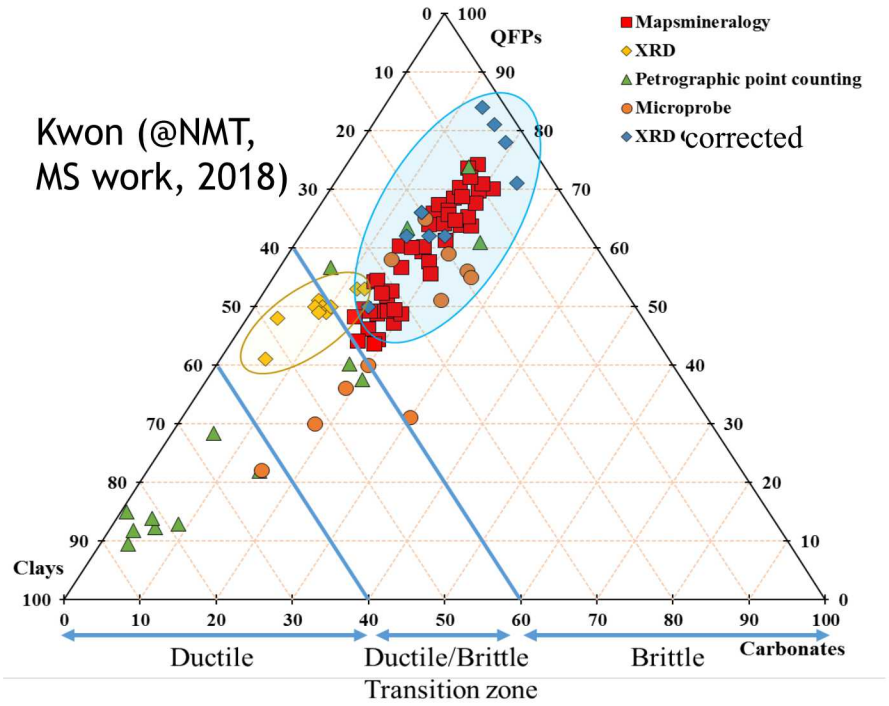

Ternary map after Ulmer-Scholle et al. (2014)

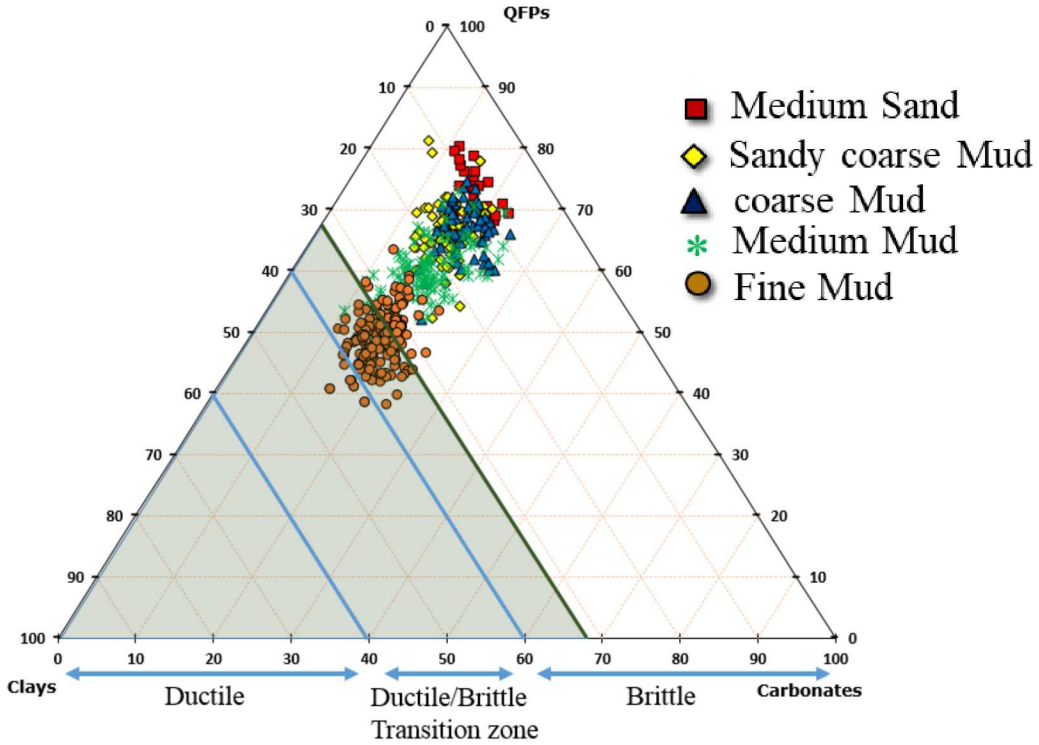

MAPS data over 50 x 50 μm^2 with 2 μm resolution

- Ternary diagram with QFPs (quartz, feldspars, pyrite), clays, and carbonates for mechanical properties (brittle to ductile)
- Petrographic point count can't distinguish fine particles/crystalline from clays
- Original XRD/microprobe analysis tend to overcount clay fraction (due to inaccurate mineral assumption and low resolution)

- MAPS data shows five micro-lithofacies that fall within a siliceous mudstone and brittle zone on the ternary diagram
- A fraction of quartz (QFPs) decreases with decreasing the grain size (clays in an opposite trend)
- Feldspars and carbonates are relatively evenly distributed

Mineralogy Mapping: Scale/methods dependent

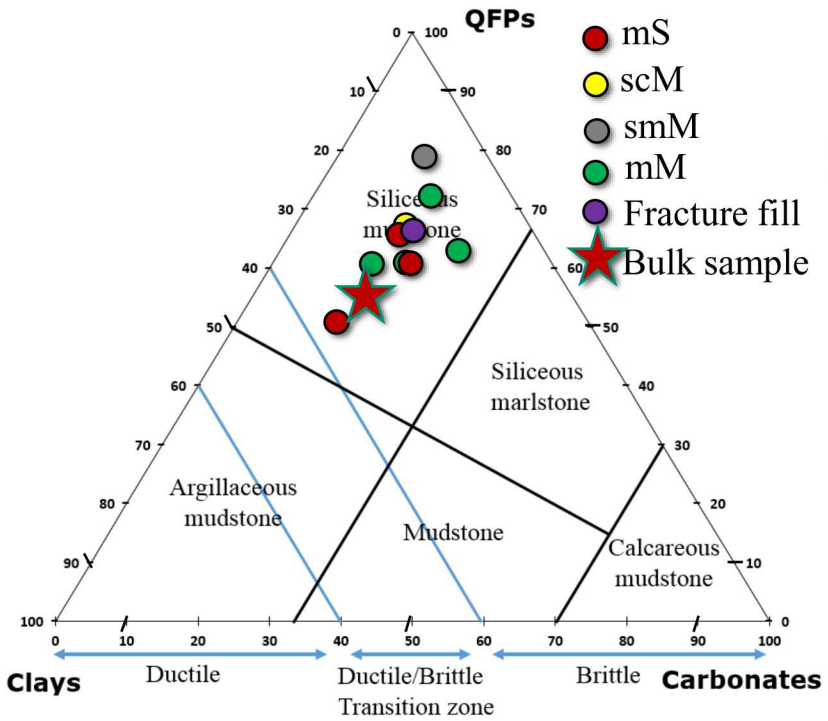

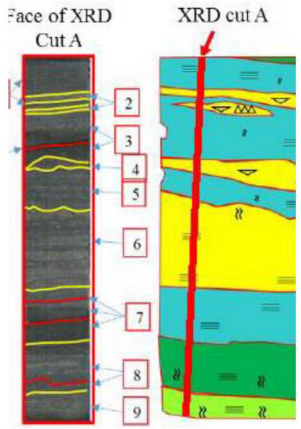

XRD (10+1 samples)

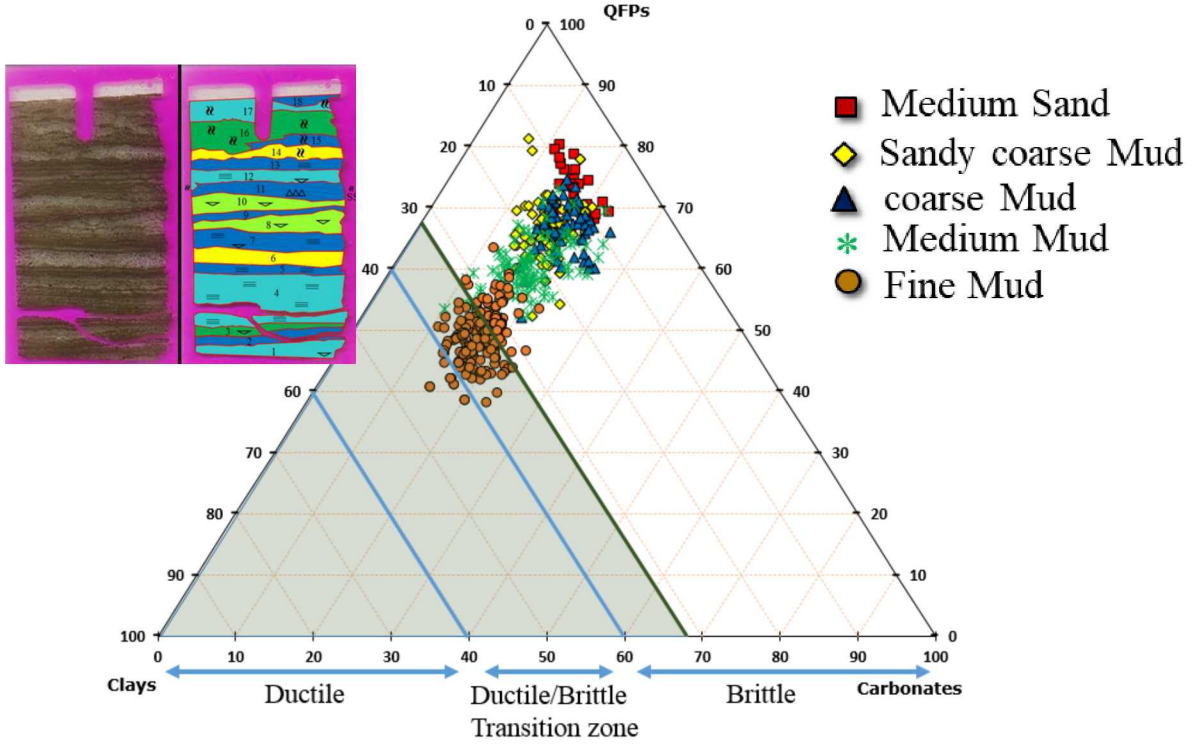

MAPS data over 50 x 50 μm^2 with 2 μm resolution

- New XRD data from 11 macroscale samples shows five micro-lithofacies that fall within a siliceous mudstone and brittle zone on the ternary diagram
- Bulk sample XRD results match MAPS data excellently

- MAPS data shows five micro-lithofacies that fall within a siliceous mudstone and brittle zone on the ternary diagram
- A fraction of quartz (QFPs) decreases with decreasing the grain size (clays in an opposite trend)
- Feldspars and carbonates are relatively evenly distributed

Yoon et al. (AAPG, Memoir 120, 2020)

Influence of geological attributes on mechanical properties

Micro-lithofacies

Medium Sand

Sandy Coarse Mud

Coarse Mud

Medium Mud

Fine Mud

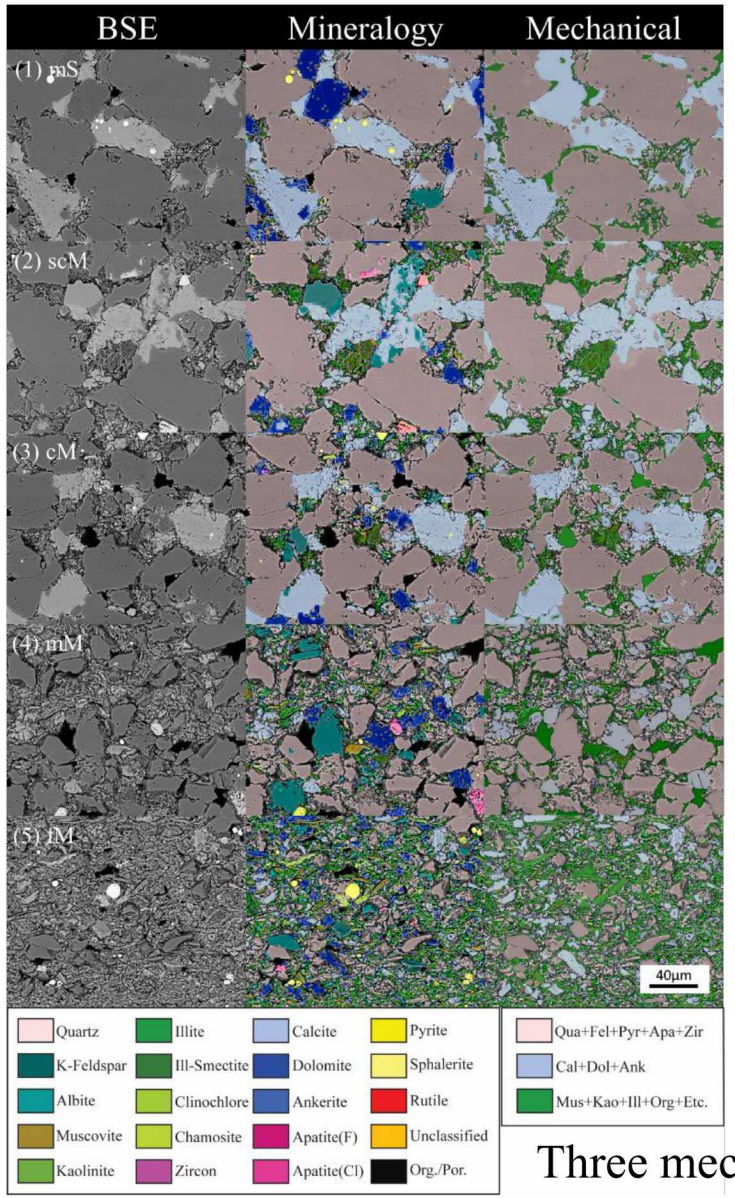

Three mechanically significant mineral assemblages

Mineral Assemblages

Mechanical properties = f(composition)? Yes

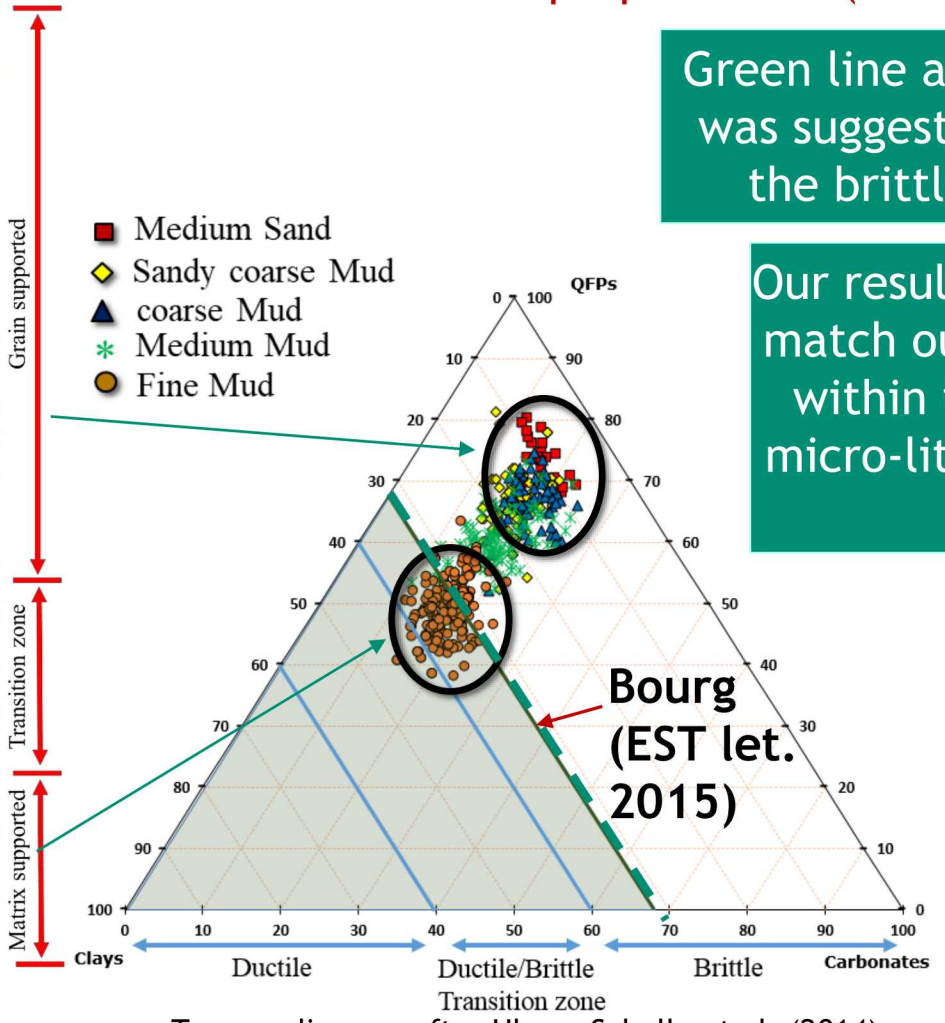

Ternary diagram after Ulmer-Scholle et al. (2014)

Green line at ~33% clays rather than ~40% was suggested (Bourg, 2015) to separate the brittle shale from sealing shale.

Our results show a clay boundary of 33% match our data better. The fine mud is within the transition zone and other micro-lithofacies are within the brittle zone.

Comparison of BSE, mineralogy, and mechanical grouping shows geological attributes would impact mechanical properties, too.

f(geological textures)? Yes

Kwon (Master degree work, NMT, 2018)

Pore Structure Characterization

- **SANS/USANS fundamental Theory**

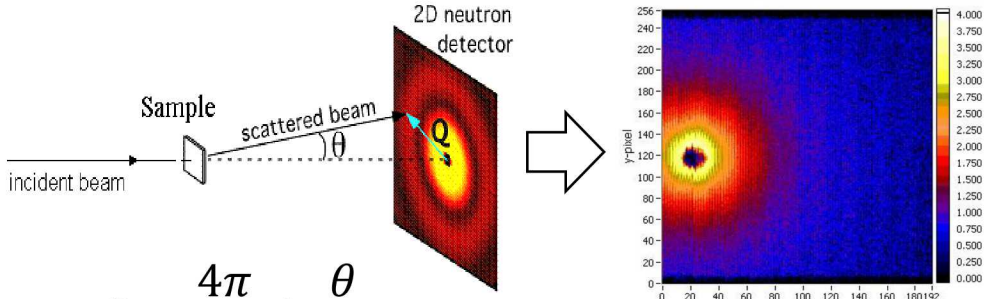

$$Q = \frac{4\pi}{\lambda}\sin\frac{\theta}{2}$$

Chemical Reaction of cement

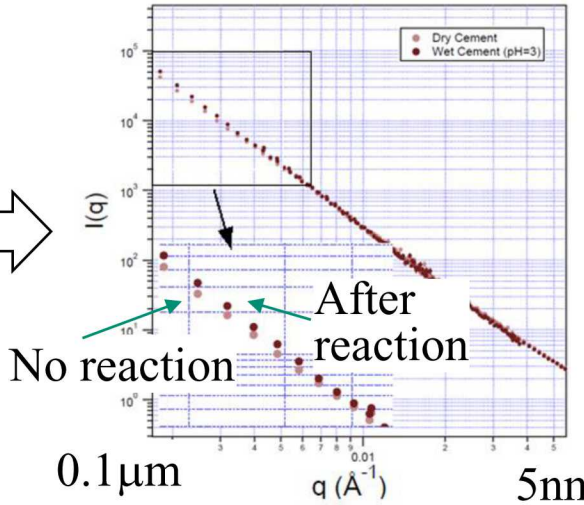

High pressure cell at NCNR

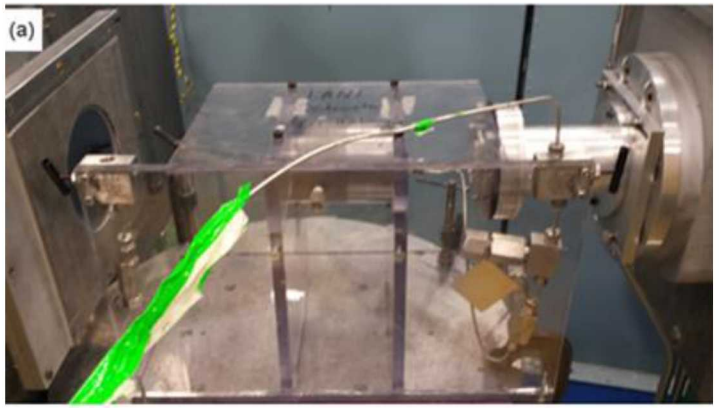

Courtesy of Dr. Rex Hjelm

- **Anisotropy**

- Pore size distribution
- Porosity
- Pore accessibility
- Specific surface area
- Fractal dimension
- Pore stability

(Liu et al., Energy&Fuel, 2019)

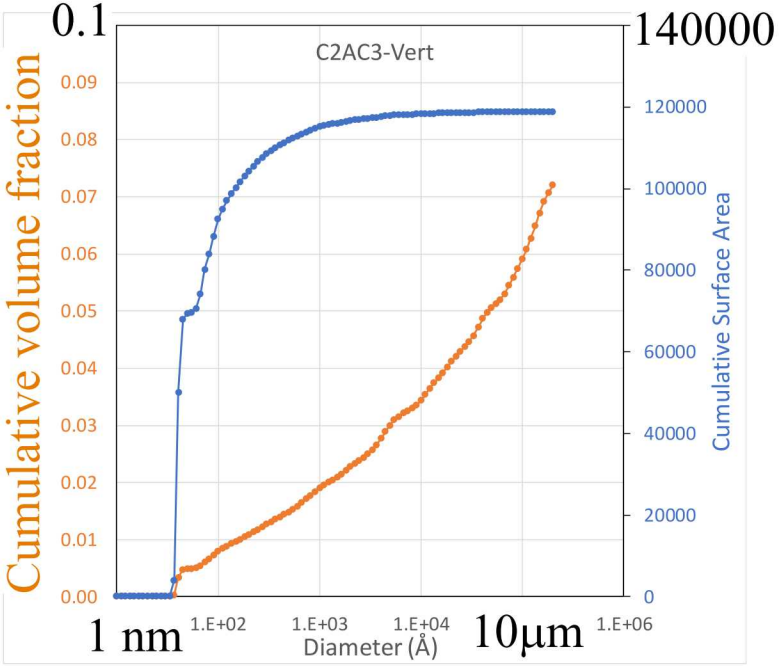

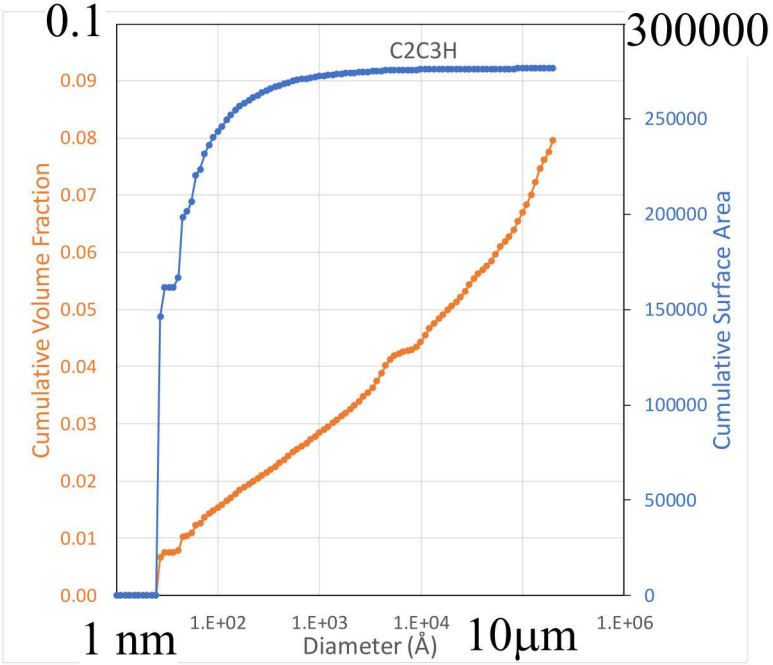

- Mineralogical and textural characterization
  - Macroscopic
  - Optical petrography/microscopy
  - Micro-CT
  - XRD/X-ray Microprobe
  - Small Angle Neutron Scattering
  - Focused Ion Beam-SEM
  - Back-Scattered Electron Microscopy
  - MAPS Mineralogy
- **Mechanical Experiments**
  - Uni-/Tri-axial compression (1x2”)
  - Brazilian Test (1x0.5”)
  - Nanoindentation
- **Computational modeling**

Conceptual Model of Anisotropic Layered System

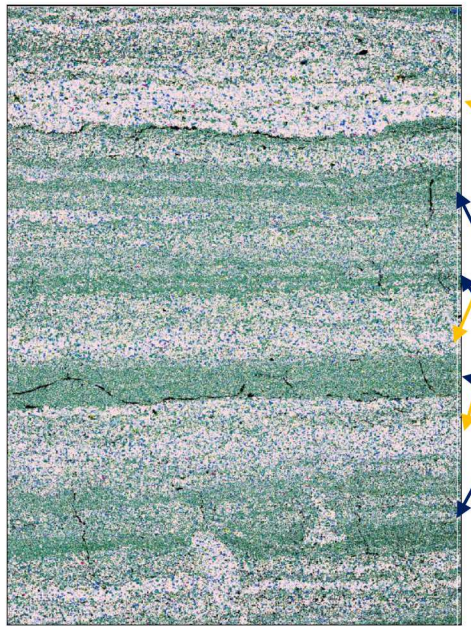

QFPs
Carbonate

Clay
Organics

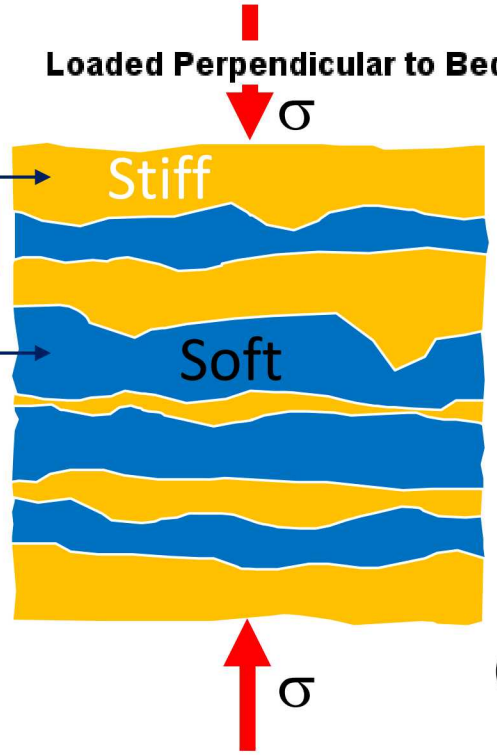

$\sigma_{stiff} = \sigma_{soft} = \sigma$

$\varepsilon_{stiff} < \varepsilon < \varepsilon_{soft}$

Overall strain

>

<

P wave velocity

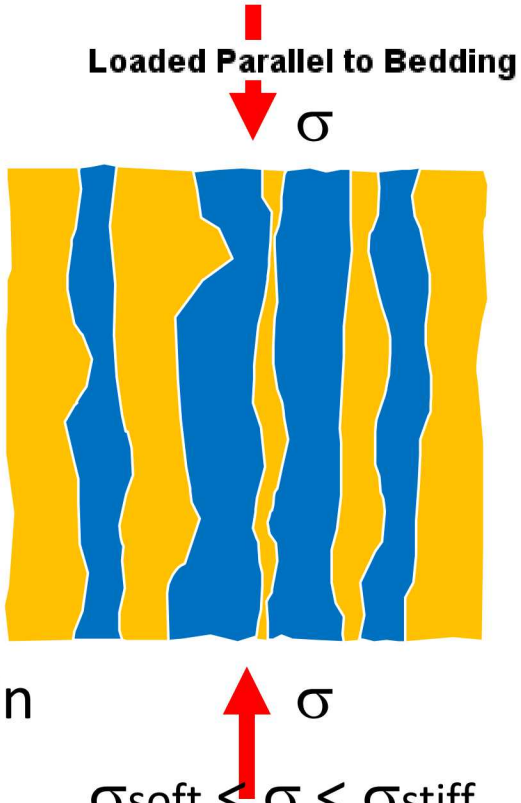

$\sigma_{soft} < \sigma < \sigma_{stiff}$

$\varepsilon_{stiff} = \varepsilon = \varepsilon_{soft}$

Axisymmetric Compression Testing

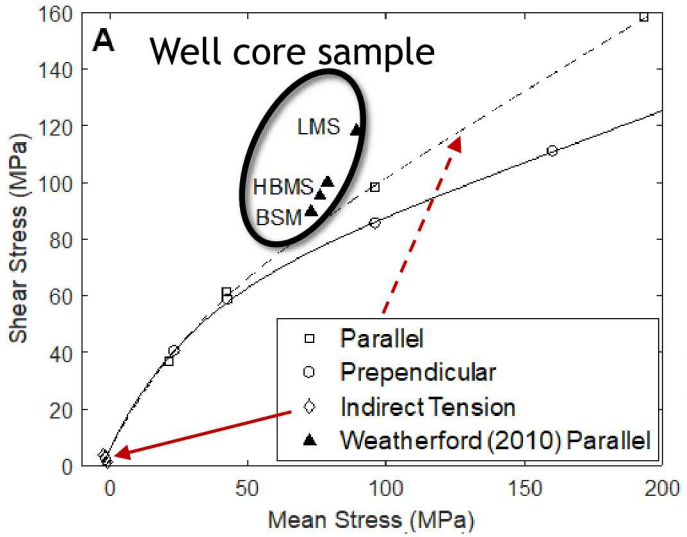

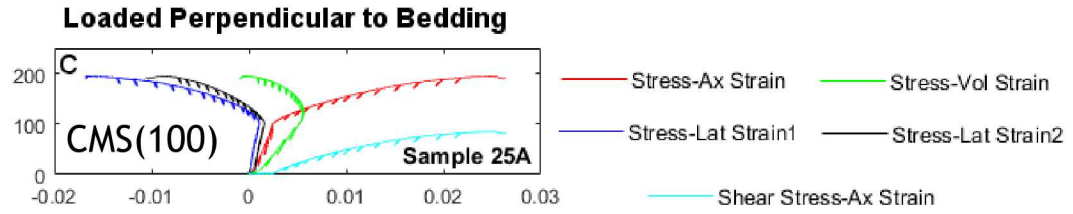

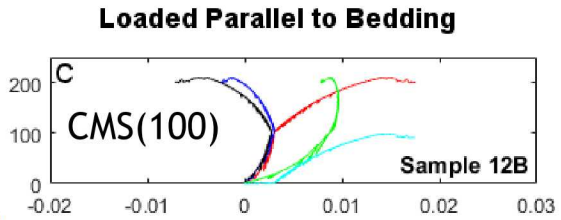

	Confined (MPa)		Axial Stress	Mean Stress	Shear Stress	Fracture Angle (v
15B	CMS (50)	Parallel	113.00	42.20	61.31	13.5
28A	CMS (50)	Perpendicular	110.64	42.80	58.75	15.5
12B	CMS (100)	Parallel	209.59	96.09	98.30	23.5
25A	CMS (100)	Perpendicular	195.07	96.20	85.62	30
14B	CMS (200)	Parallel	376.37	193.42	158.44	27.5
22A	CMS (160)	Perpendicular	288.64	160.31	111.14	35.5

CMS: Constant Mean Stress

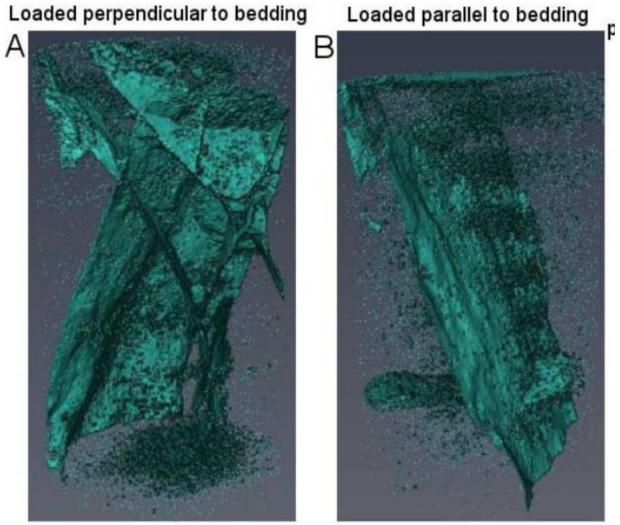

Segmented MicroCT images of failed samples

Yoon et al. (AAPG, Memoir 2019, in press)

Axisymmetric Compression Testing

Horizontal slice through the central part of sample

One primary & two secondary fractures

A. Loaded parallel to bedding (15B)

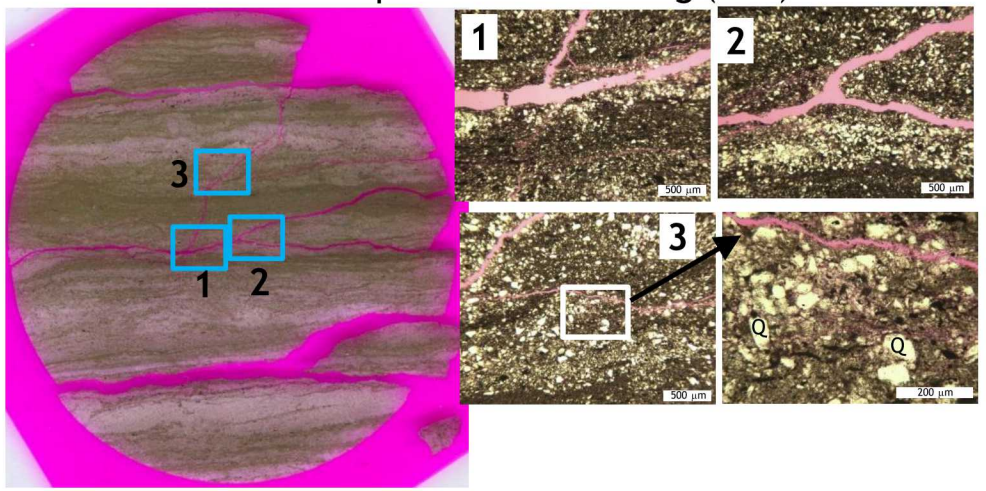

Fracture intersection & bifurcation with small aperture microfractures

Microfracture propagation in between quartz grains

B. Loaded perpendicular to bedding (28A)

Curved main fracture

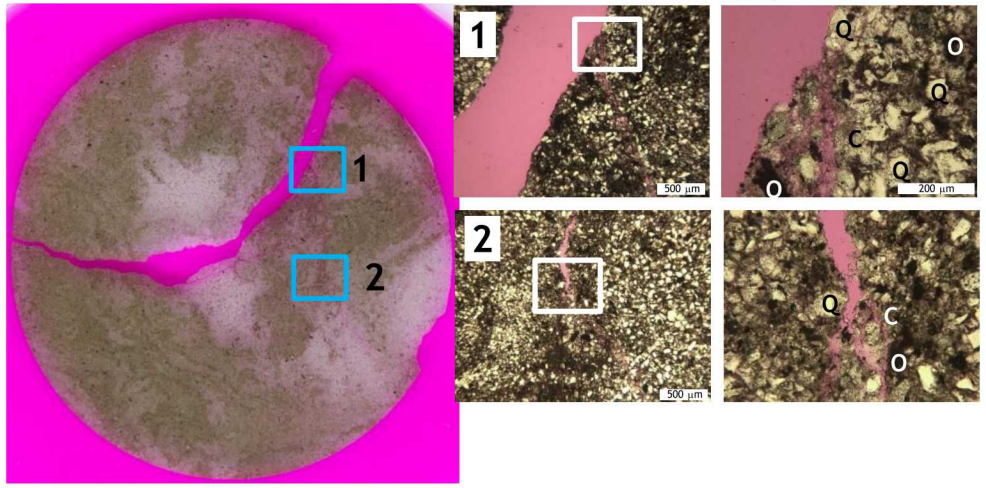

Microfracture patterns in between quartz grains

Indirect Tension Testing

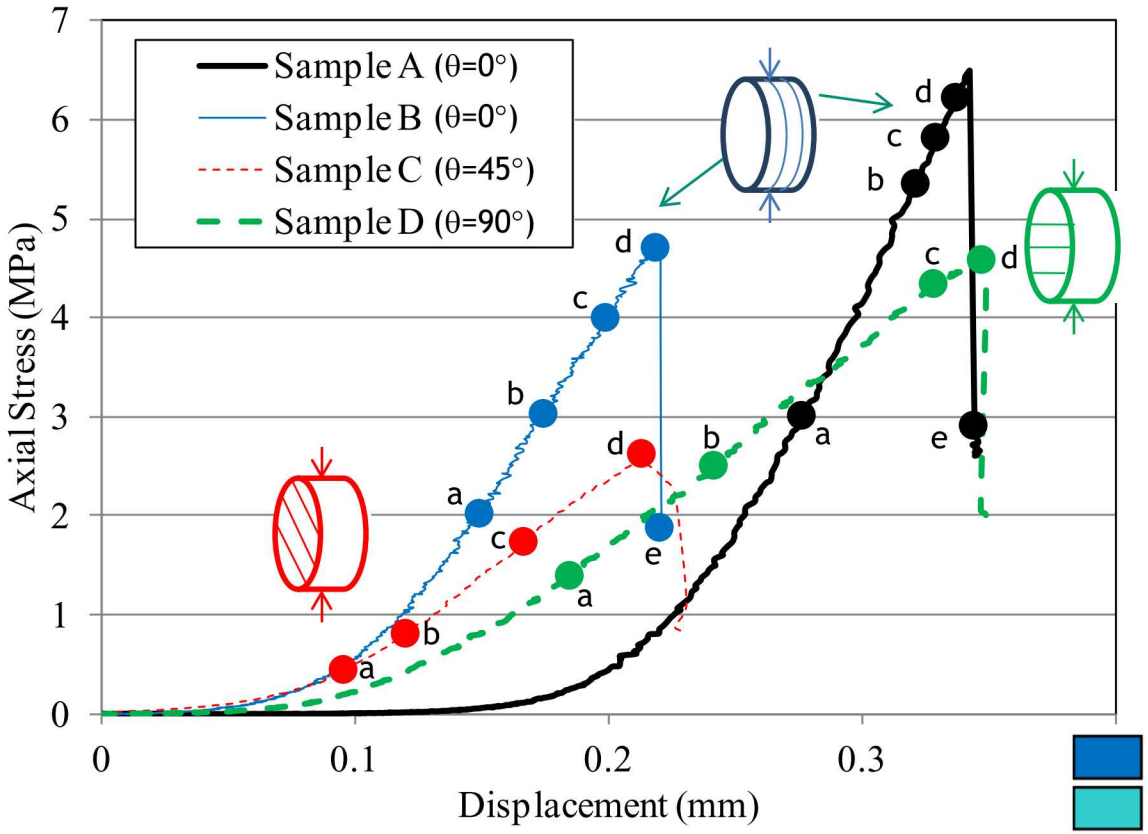

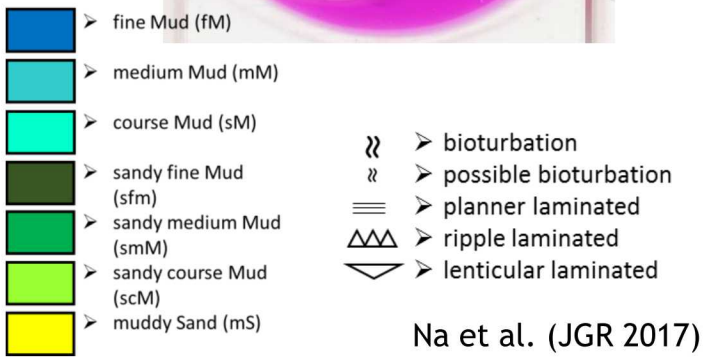

Na et al. (JGR 2017)

$$\sigma_t = \frac{2P}{\pi D t}$$

P: Loading

D: Diameter

t: thickness

Numerical Simulations of Brittle Fracturing

Crack phase field (φ)

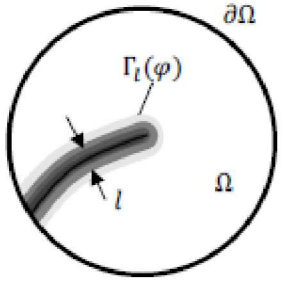

- Phase field model for crack representation
- Shale is modeled as two-constituent brittle materials with stiff and soft layers:
  - Young's Modulus
  - (Pore pressure)
  - (Chemo-mechanical coupling)

DEAL.II Open Source Finite Element Library

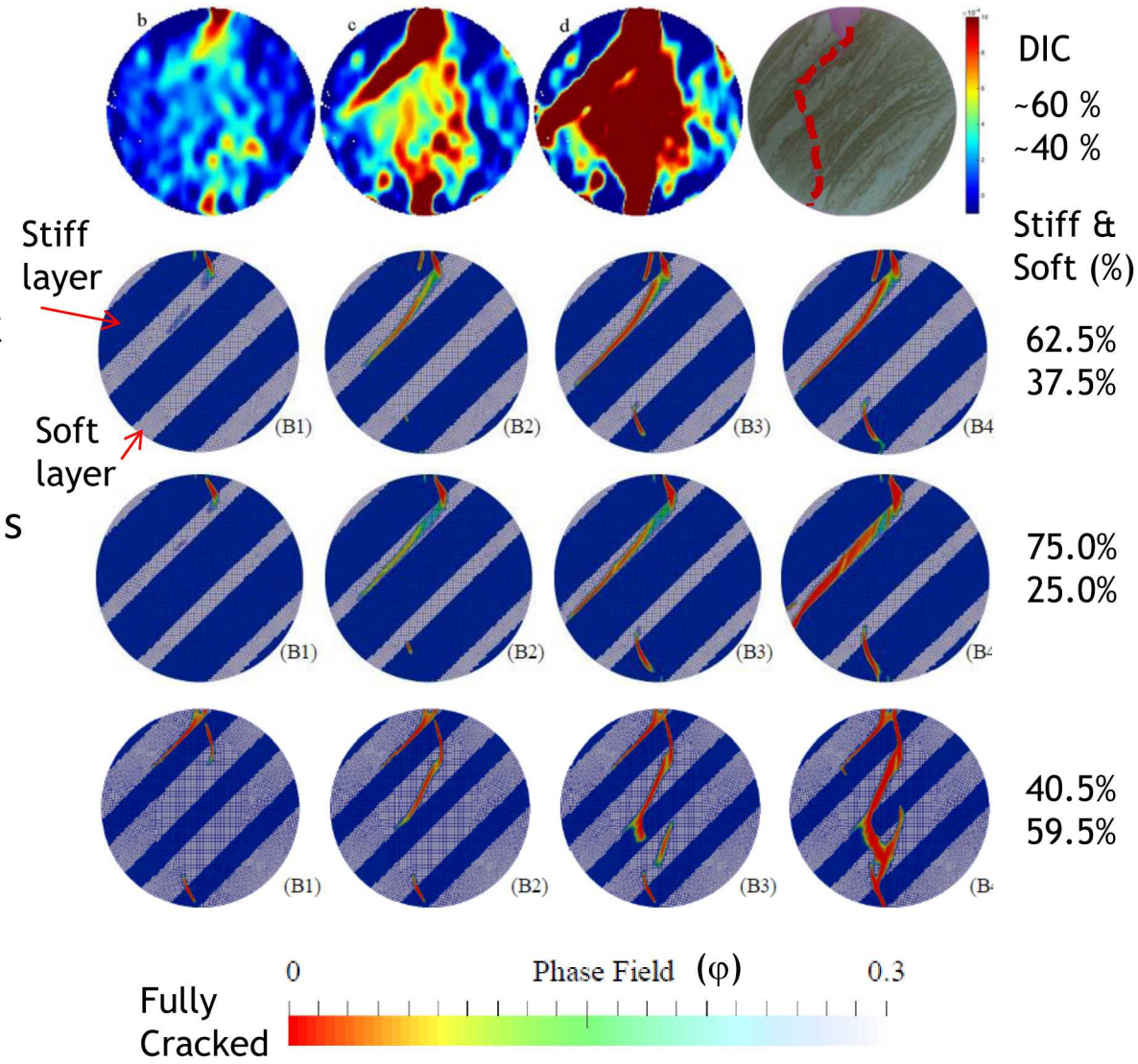

Na et al. (JGR 2017)

Effective Properties of Heterogeneous Materials

- Transversely isotropic effective medium for elastic parameters (Berryman, 1998)
  - Spatial homogenization procedure leads to much simpler crack patterns than those from the layered isotropic materials
  - Smaller surface area created by the fracture process yields the reduced tortuous crack paths with a diminished amount of energy dissipation (much higher effective fracture toughness)
  - Crack paths in the effective medium are less tortuous due to (probably) filtering out mesoscopic information via homogenization

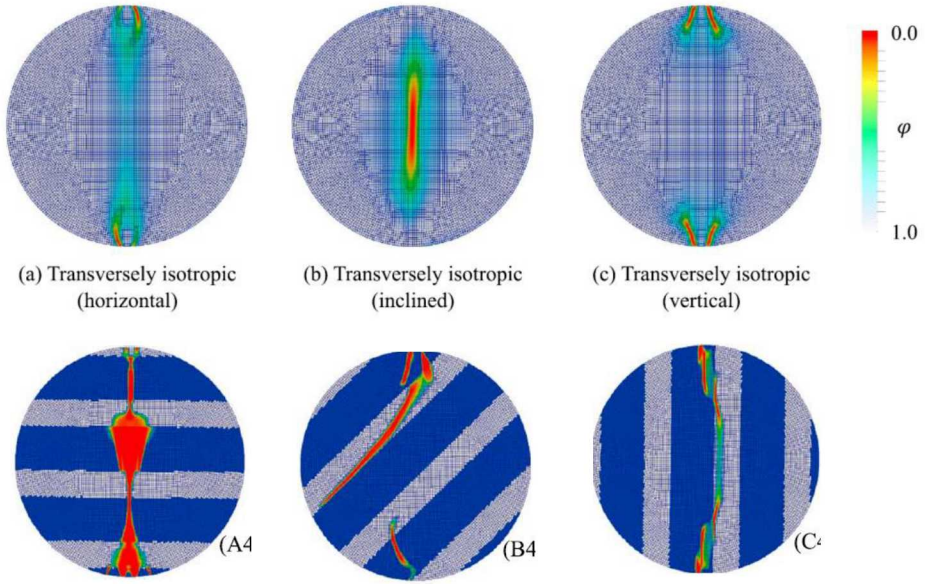

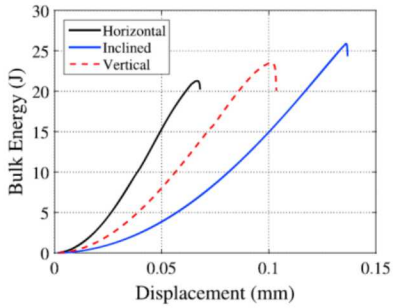

Transversely Isotropic

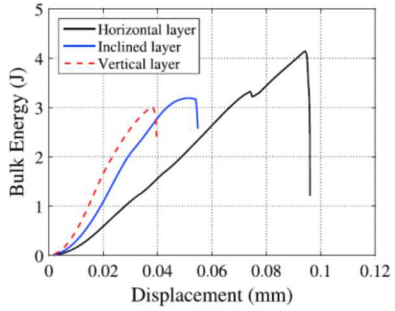

Layered Isotropic

Na et al. (JGR 2017)

- Mineralogical and textural characterization
  - Macroscopic
  - Optical petrography/microscopy
  - Micro-CT
  - XRD/X-ray Microprobe
  - Small Angle Neutron Scattering
  - Focused Ion Beam-SEM
  - Back-Scattered Electron Microscopy
  - MAPS Mineralogy
- Mechanical Experiments
  - Uni-/Tri-axial compression (1x2”)
  - Brazilian Test (1x0.5”)
  - Nanoindentation
- Computational modeling

Nanoindentation

- **Depth sensing/instrumented indentation**
  - highly accurate load-displacement record
  - Analytical models to determine modulus, hardness and other mechanical properties using the load-displacement data

- **Analytical concept**
  - Purely elastic deformation upon initial unloading
  - Compliance of the sample and indenter tip - springs in series
  - Hardness = load/contact area
  - Elastic modulus determined by stiffness (S)

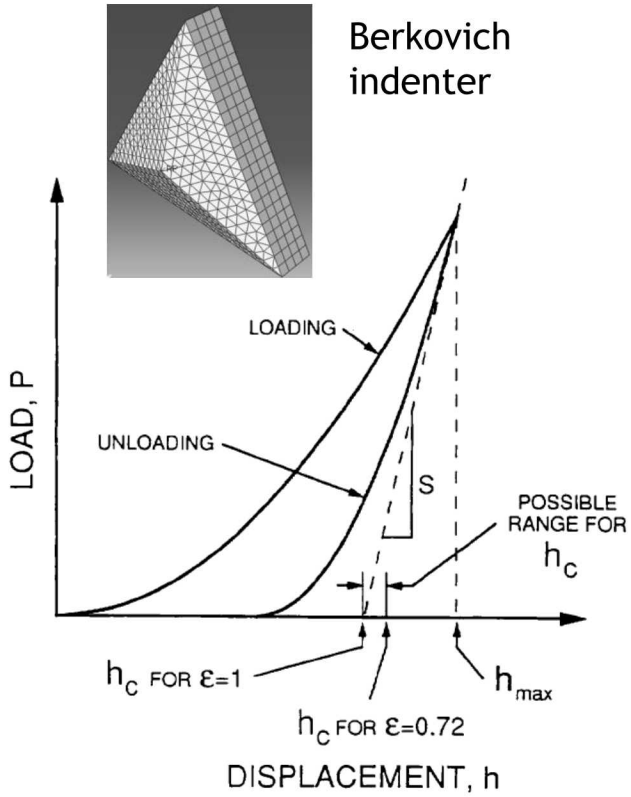

Oliver & Pharr (1992)

[Hysitron TriboIndenter 900]
Indentation strain rate = 0.1 (Oliver et al., 1997)
(current change in displacement/current total disp.)
Maximum load = 0.1,1 10 mN (multiscale indenting)
A total of >1500 indentations were performed.

Multiscale Nanoindentation Results

As expected, variations of indentation results decrease with increasing the scale. Indentation results at the scale (iii) show the representative elemental volume (REV).

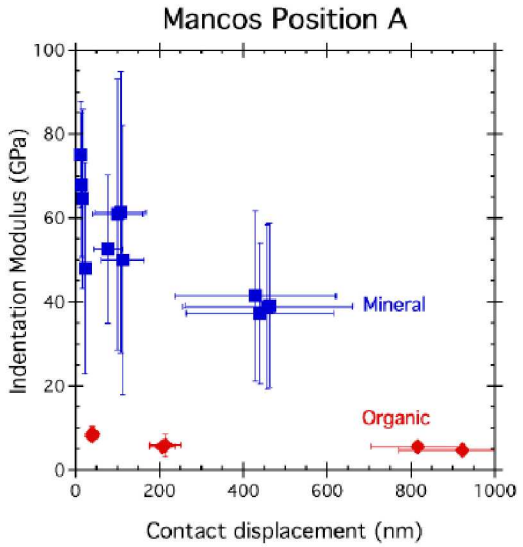

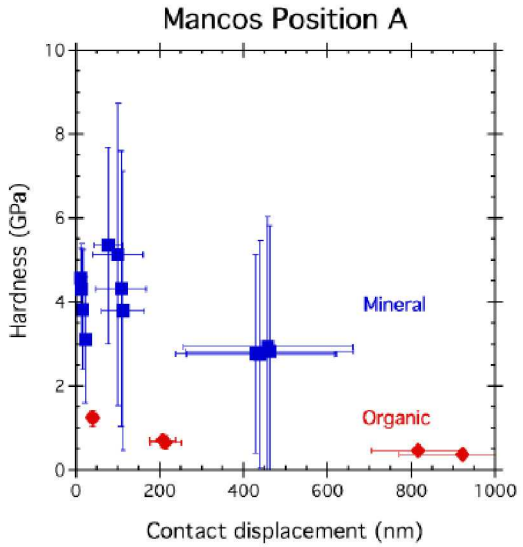

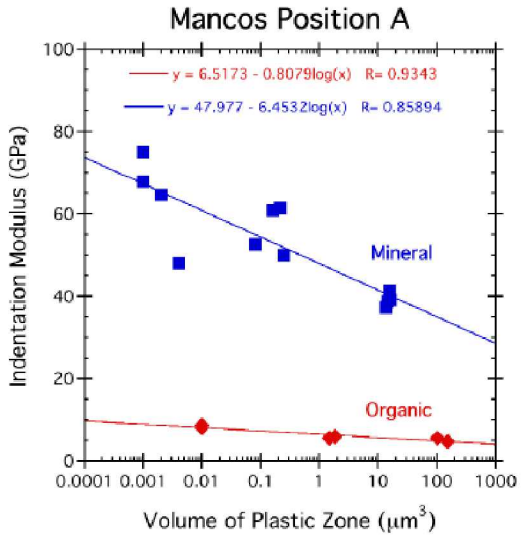

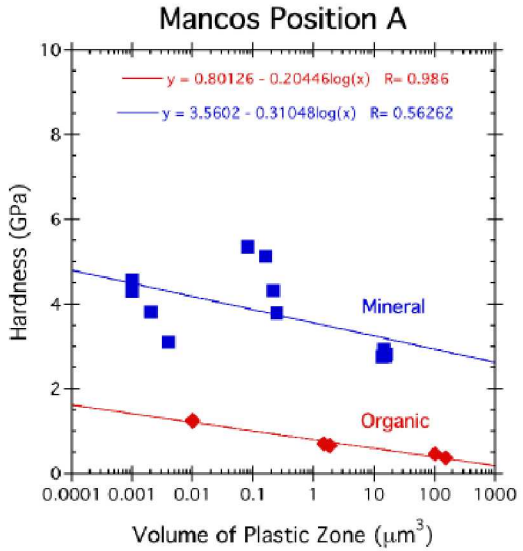

Distributed arrays

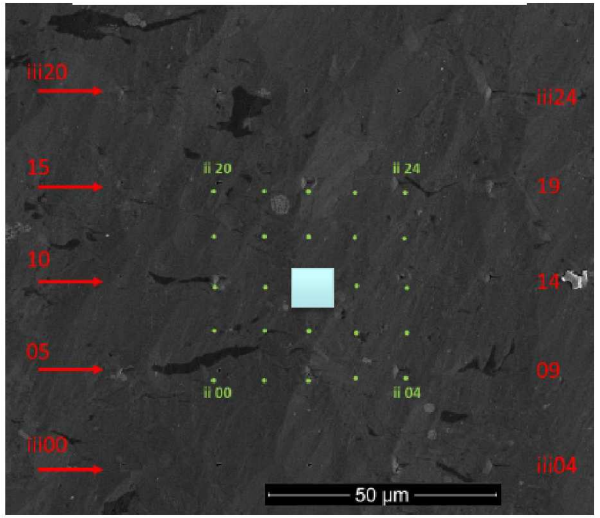

Indentation key	Array dimension	indent spacing	Max Load
i	8x8 um	2 um	0.1 mN
ii	40x40 um	10 um	1 mN
iii	80x80 um	20 um	10 mN

Estimate plastic zone radius

$$\frac{R_p}{\delta_m} = -12.907\frac{H}{E_r} + 4.5451 \qquad \frac{H}{E_r} < 0.35$$

Chen & Bull, Surface & Coatings Technology (2006) 4289–4293.

Nanoindentation Impressions

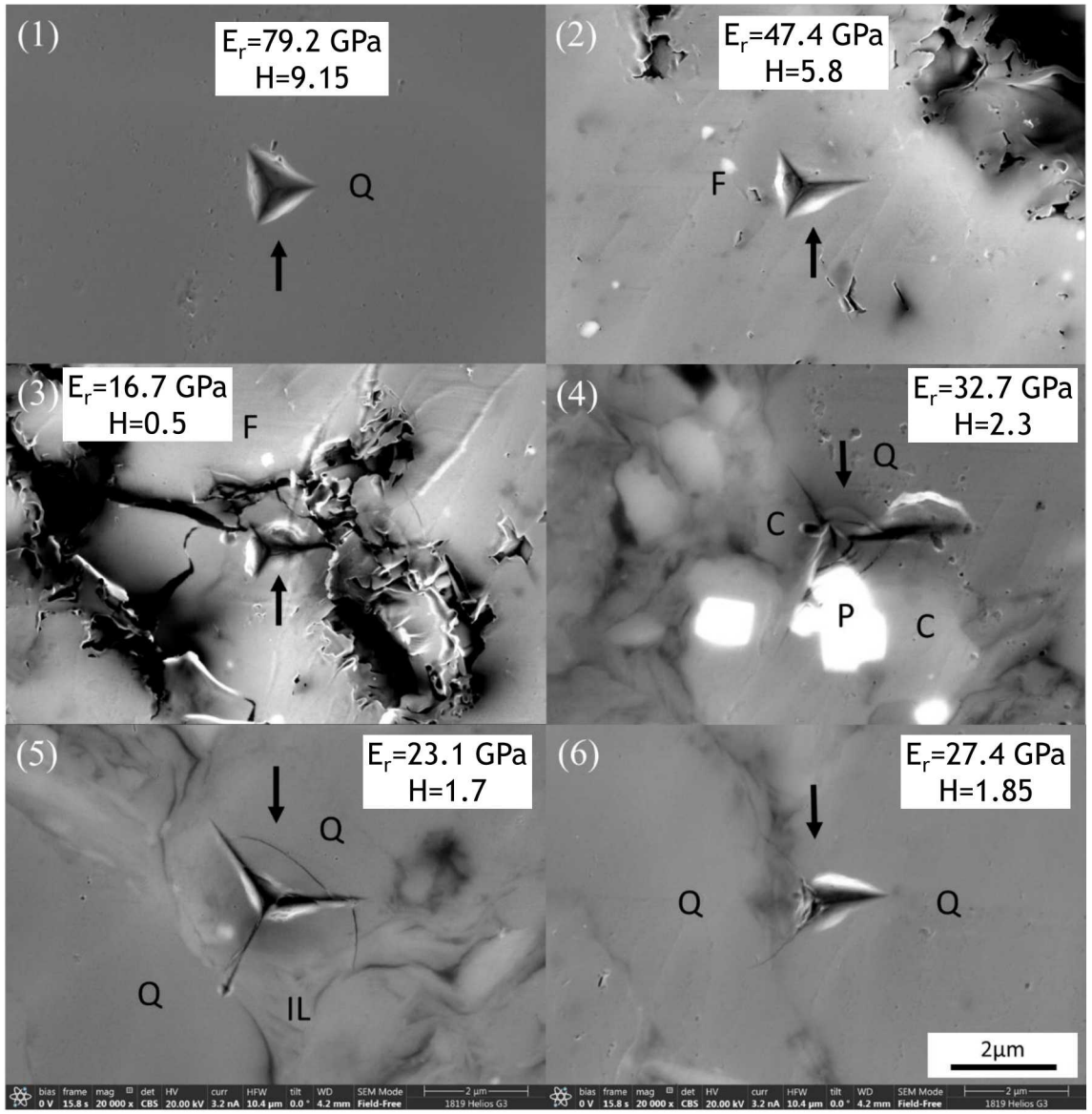

NOTE: Q=quartz, P=pyrite, C=carbonate, F=feldspar, and IL=illite)

(1-2) Low-clay contents: surface of pure quartz and feldspar having higher values of mechanical properties such as elastic modulus and hardness

(3) Dissolution surface of feldspar (mechanical properties are weaker)

(4-6) Grain-to-grain boundary and edge-of-grain, which have lower mechanical properties values

Variations of measured modulus at low clay contents came from geological textures such as boundary of grains, dissolution of grain etc. that are likely to form during diagenesis. These results indicate the important role of geological attributes in mechanical properties of mudstone.

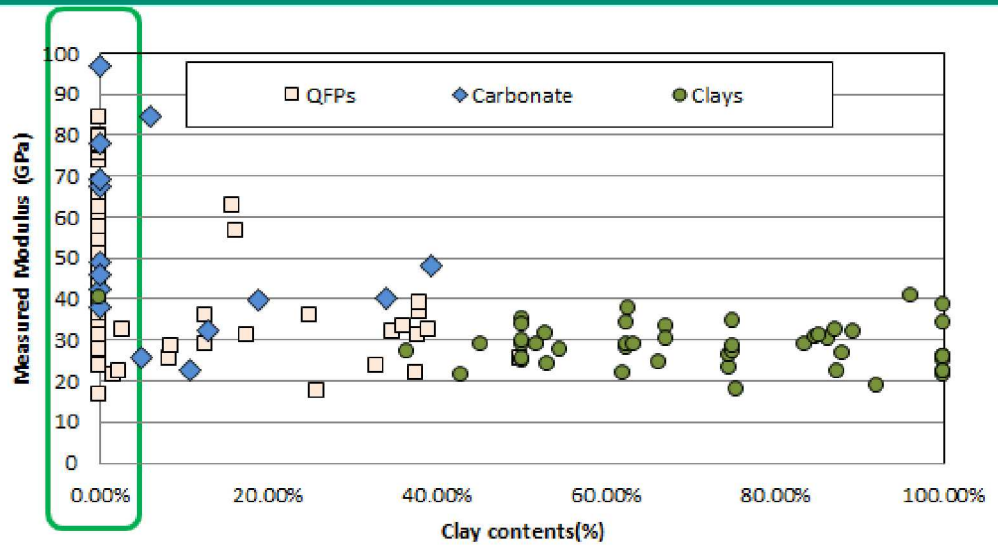

Simulation of Nanoindentation

Model setup

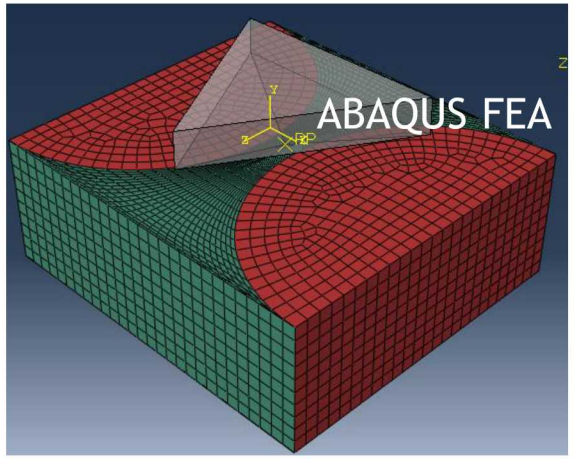

Indentation impression

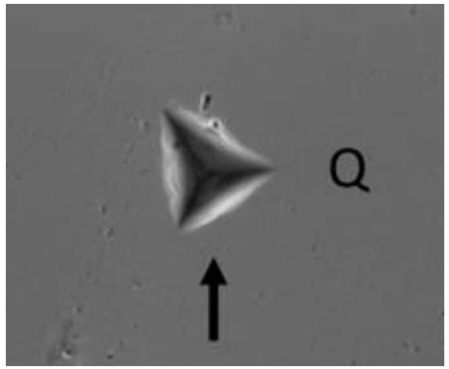

Simulated Indentation mark

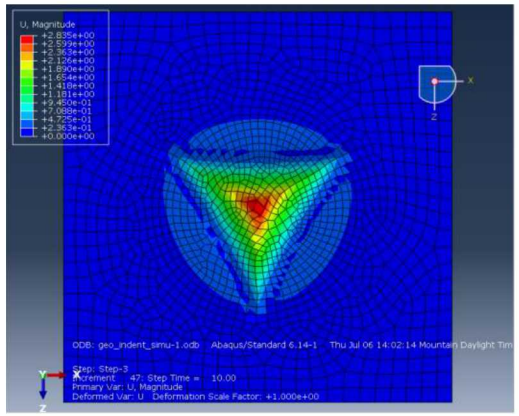

Force vs. Displacement

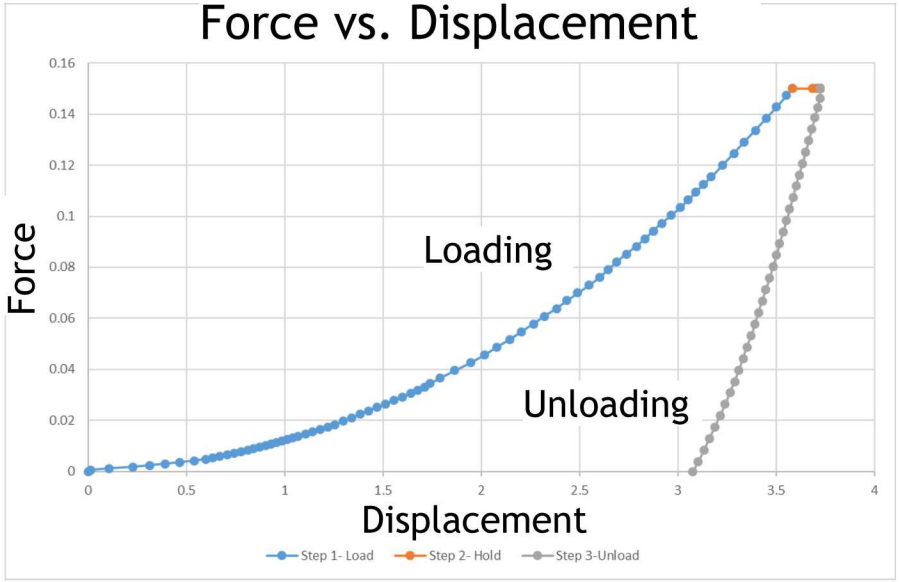

Elastic Modulus

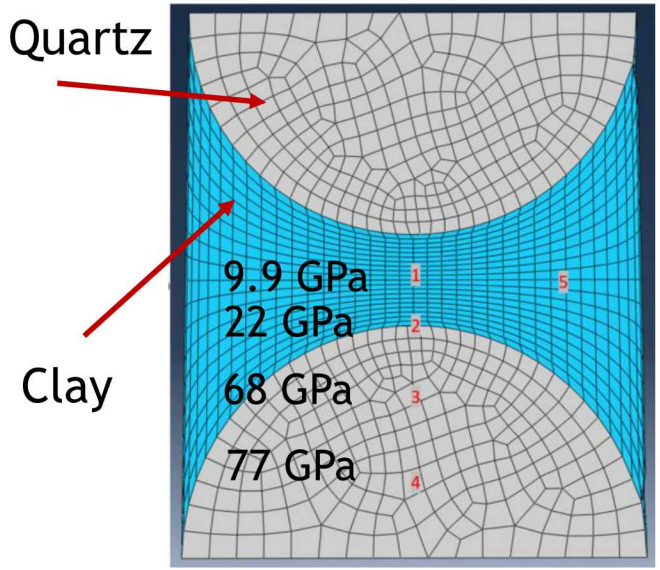

- Numerical simulations were performed with a Berkovich indenter
- Simulation has three steps including loading, holding, and unloading steps to mimic actual indentation setup
- Simulated indentation mark mimics an ideal indentation mark on quartz well
- Simulation results clearly show that calculated elastic modulus at different locations from the center of quartz to clay decrease
- This clearly demonstrates that the precise location of indentation (in other words, compositional heterogeneity) impacts estimated mechanical properties signficantly

Upscaling for Mechanical Properties

- Phase field modeling for averaging mechanical properties
  - Spatial mineralogical mapping with compositional heterogeneity
  - Development of correlation with nanoindentation results
  - Evaluation of soft cement or multi-mineral regions on mechanical responses with various conditions (e.g., defects, layering, anisotropy)

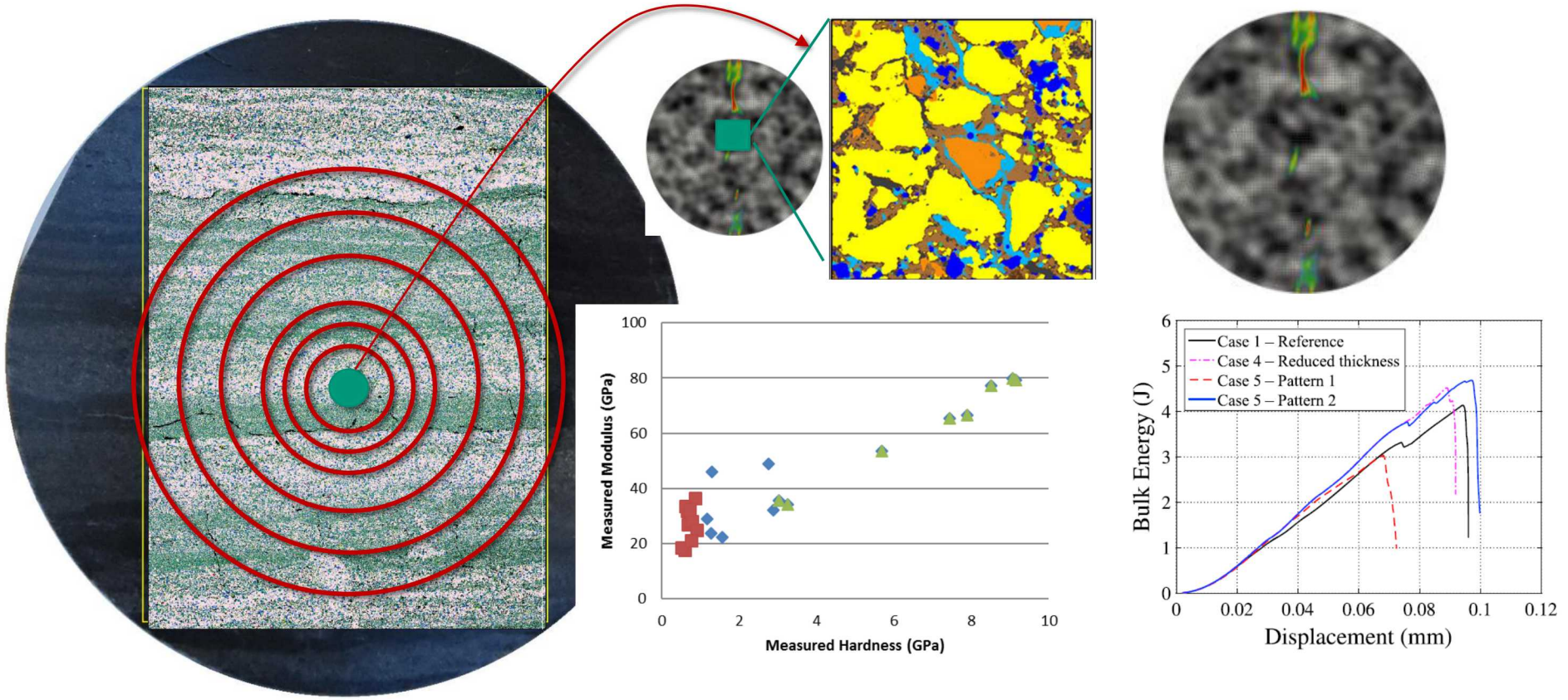

Velocities of Mancos Shale lithofacies

Drilled Core Samples

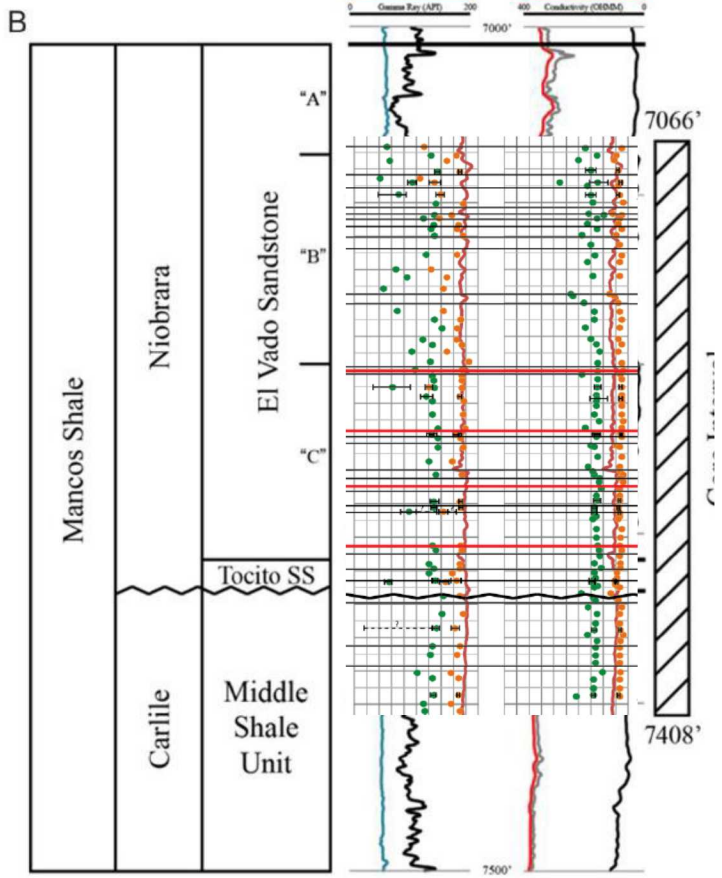

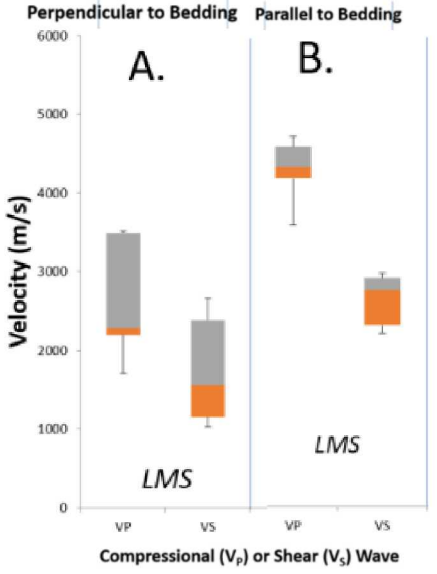

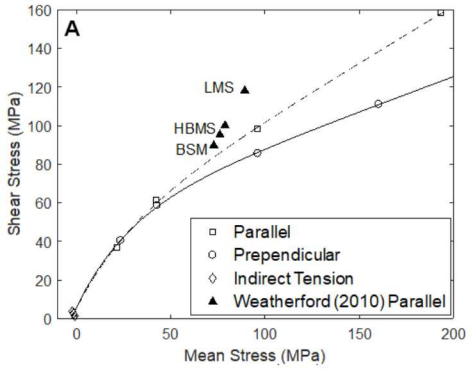

Lab Block Samples

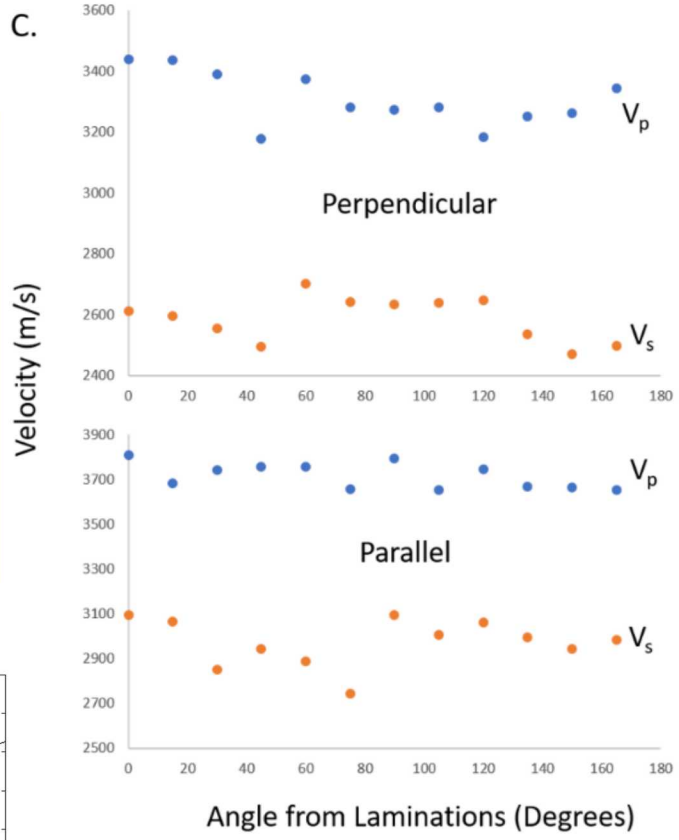

Machine Learning Applications

Image segmentation

3D images (FIB-SEM) & TEM/EDX

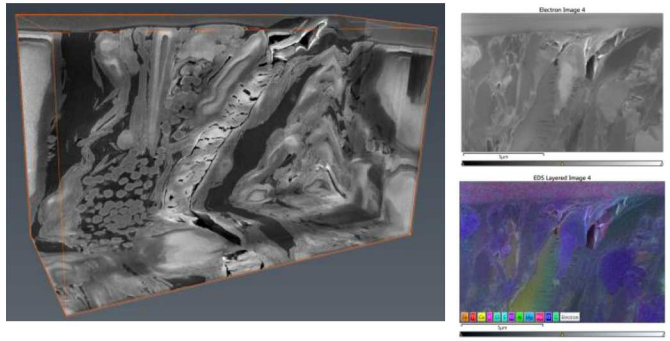

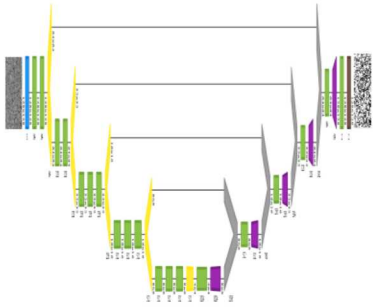

U-Net architecture with U-Net, VGG16, ResNet etc.

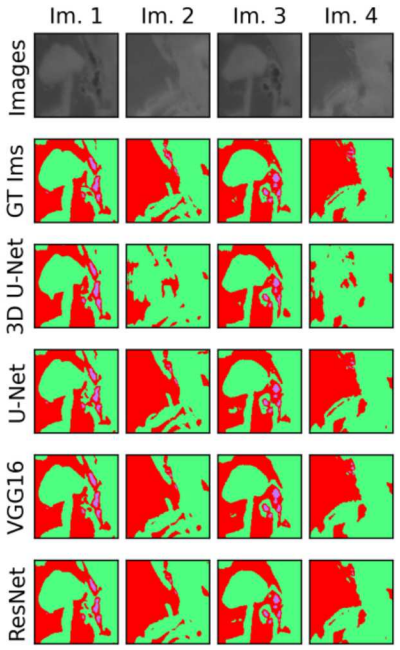

Mineral Identification

1” Brazilian Test Sample & MAPS data

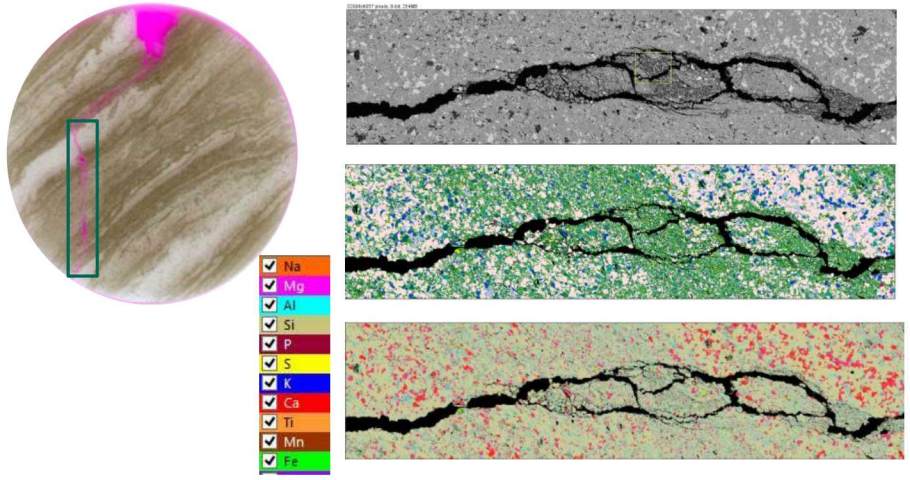

Multilabel classification

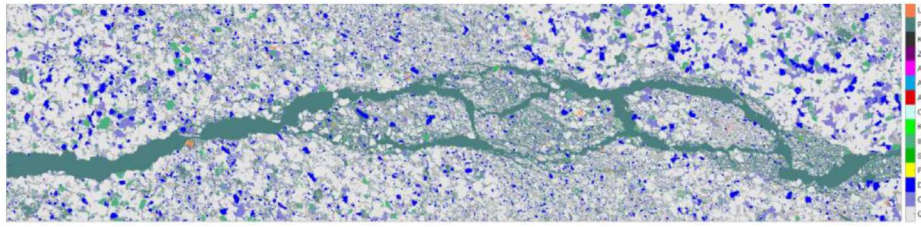

Convolutional neural network-based multi-label classification
Input data: 15 elemental maps, elemental distribution ratio, BSE image
Output: multiple minerals per pixel

Digital Rock Generation

Deep Convolutional Generative Adversarial Network (DCGAN)

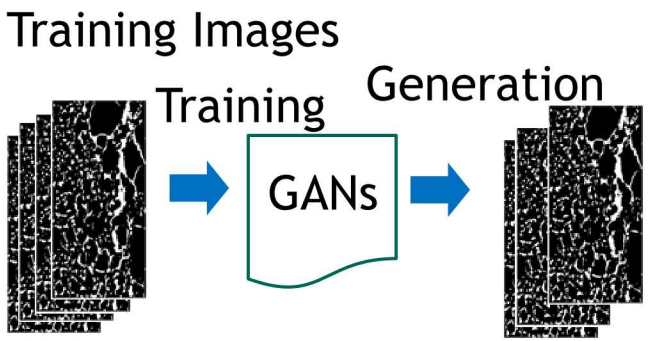

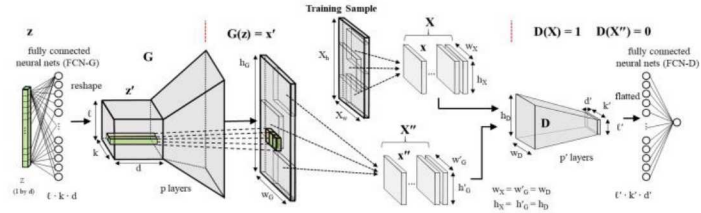

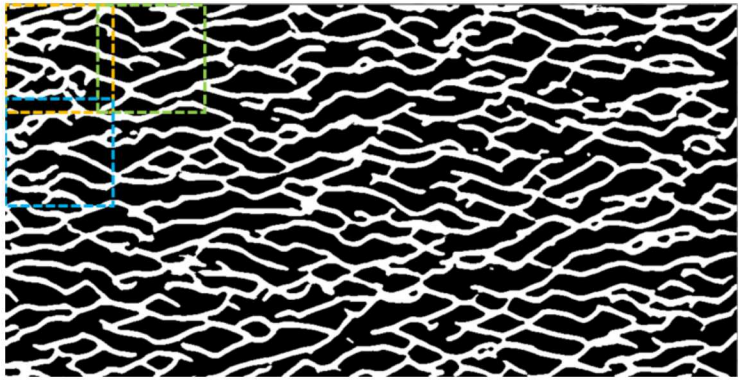

Summary & Conclusions

- Integrated multiscale imaging and mechanical testing with numerical simulation was used to advancing our understanding of mechanical properties of Mancos shale
- Texture/mineralogical characterization
  - Recent advances in mineralogical mapping with high resolution imaging over the large area
  - Multiscale mineralogical and geologic features lead to considerable heterogeneity of mechanical properties
- Mechanical characterization
  - Both mineralogy and its distribution govern distinctively different mechanical properties
  - Mechanical map and nanoindentation test suggest the important role of geological attribute to mechanical properties of mudstone
  - Microscopic heterogeneity of mechanical properties can control the spatial distribution of fractures
  - This heterogeneity should be taken into account for realistic mechanical modeling and can scale up by rigorous theoretical and numerical modeling

Key reference: Yoon et al., 2020, Impact of depositional and diagenetic heterogeneity on multiscale mechanical behavior of mancos shale, New Mexico and Utah, USA, in W. Camp, K. Milliken, K. Taylor, N. Fishman, P. Hackley, and J. Macquaker, eds., Mudstone diagenesis: Research perspectives for shale hydrocarbon reservoirs, seals, and source rocks: AAPG Memoir 120. Chapter 8 p. 121–148. [if there is any question including the preprint version of the chapter, please contact hyoon@sandia.gov]